

# FINITE-SIZE AND CORRELATION-INDUCED EFFECTS IN MEAN-FIELD DYNAMICS

JONATHAN TOUBOUL<sup>†‡</sup> AND G. BARD ERMENTROUT<sup>†</sup>

**Abstract.** The brain's activity is characterized by the interaction of a very large number of neurons that are strongly affected by noise. However, signals often arise at macroscopic scales integrating the effect of many neurons into a reliable pattern of activity. In order to study such large neuronal assemblies, one is often led to derive mean-field limits summarizing the effect of the interaction of a large number of neurons into an effective signal. Classical mean-field approaches consider the evolution of a deterministic variable, the mean activity, thus neglecting the stochastic nature of neural behavior. In this article, we build upon a recent approach that includes correlations and higher order moments in mean-field equations, and study how these stochastic effects influence the solutions of the mean-field equations, both in the limit of an infinite number of neurons and for large yet finite networks. We show that, though the solutions of the deterministic mean-field equation constitute uncorrelated solutions of the new mean-field equations, the stability properties of limit cycles are modified by the presence of correlations, and additional non-trivial behaviors including periodic orbits appear when there were none in the mean field. The origin of all these behaviors is then explored in finite-size networks where interesting mesoscopic scale effects appear. This study leads us to show that the infinite-size system appears as a singular limit of the network equations, and for any finite network, the system will differ from the infinite system.

**Key words.** Neural Mass Equations; Dynamical Systems; Markov Process; Master Equation; Moment equations; Bifurcations; Wilson and Cowan system.

**AMS subject classifications.** 92B25,65P30,37M20,34C05,34C23,34C60,92B20,92C20

**Introduction.** Cortical activity manifests highly complex behaviors which is often strongly characterized by the presence of noise. Reliable responses to specific stimuli often arise at the level of population assemblies (cortical areas or cortical columns) featuring a very large number of neuronal cells presenting a highly nonlinear behavior and that are interconnected in a very intricate fashion. Understanding the global behavior of large-scale neural assemblies has been a great endeavor in the past decades. Most models describing the emergent behavior arising from the interaction of neurons in large-scale networks have relied on continuum limits ever since the seminal work of Wilson and Cowan and Amari [2, 3, 38, 39]. Such models tend to represent the activity of the network through a macroscopic variable, the population-averaged firing rate, that is generally assumed to be deterministic. Many analytical and numerical results and properties have been derived from these equations and related to cortical phenomena, for instance for the problem of spatio-temporal pattern formation in spatially extended models (see e.g. [14, 17, 19, 25]).

This approach tends to implicitly make the assumption that correlations in the activity do not modify the behavior of the system in large populations. However, the stochasticity of the system, and in particular the presence of correlations in the activity may considerably affect the dynamics in such nonlinear systems, and these can be even more important as the network size increases. These models therefore make the assumption that averaging effects counterbalance the prominent noisy aspect of *in vivo* firing, a feature that can dramatically affect finite-sized network activity, and, thus, that the emergent behavior of a cortical column is deterministic.

---

<sup>†</sup>Department of Mathematics, University of Pittsburgh, Pittsburgh PA, USA

<sup>‡</sup>NeuroMathComp Laboratory, INRIA, Sophia Antipolis, France

jonathan.touboul@sophia.inria.fr

However, increasingly many researchers now believe that the different intrinsic or extrinsic noise sources are part of the neuronal signal, and rather than a pure disturbing effect related to the intrinsically noisy biological substrate of the neural system, they suggest that noise conveys information that can be an important principle of brain function [32]. At the level of a single cell, various studies have shown that the firing statistics are highly stochastic with probability distributions close to Poisson distributions [33], and several computational studies confirmed the stochastic nature of single-cells firings [11, 30, 35, 36]. How variability at the single neuron level affects dynamics of cortical networks is less established so far. Theoretically, the interaction of a large number of neurons that fire stochastic spike trains can naturally produce correlations in the firing activity of the population considered. For instance power-laws in the scaling of avalanche-size distributions has been studied both via models and experiments [5, 6, 26, 34]. In these regimes the randomness plays a central role.

A different approach has been to study regimes where the activity is uncorrelated. A number of computational studies on the integrate-and-fire neuron showed that under certain conditions neurons in large assemblies end up firing asynchronously, producing null correlations [1, 4, 10]. In these regimes, the correlations in the firing activity decrease towards zero in the limit where the number of neurons tends to infinity. The emergent global activity of the population in this limit is deterministic, and evolves according to a mean-field firing rate equation. However, these states only exist in the limit where the number of neurons is infinite, and such asynchronous states do not necessarily exist in cortical areas or in computational models, and even when they exist, they are not necessarily stable. This raises the question of how the finiteness of the number of neurons impacts the behavior of asynchronous states, and how to study non-asynchronous behaviors. The study of finite-size effects in the case of asynchronous states is generally not reduced to the study of mean firing rates and can include higher order moments of firing activity [28, 16, 9]. In order to go beyond asynchronous states and take into account the stochastic nature of the firing and how this activity scales as the network size increases, different approaches have been developed, such as the population density method and related approaches [13]. Most of these approaches involve expansions in terms of the moments of the resulting random variable, and the moment hierarchy needs to be truncated which is a quite hard task that can raise a number of technical issues (see e.g.[27]). A recent approach overcomes this truncation difficulty by considering the mean-field behavior as a stochastic process and therefore treating the rigorous limit equation of the interaction of many stochastic neurons as a fixed point equation in the space of stochastic processes, making use of the powerful tools of stochastic limit theorems and large deviation techniques (see [20]).

The present manuscript will focus on the comparison of two recently developed stochastic models with the customary Wilson and Cowan equations. These two models draw upon a framework recently developed by El Boustani and Destexhe [16] where the firing at the level of each neuron is considered to be a Markov variable that depends on the state of the network. The transition probability of this chain is modelled to satisfy a differential equation called *master equation* of the system. The global resulting activity is then readily derived from the activity of all neurons in the network. The two models of interest here were instantiated specifically in order to be compared to standard Wilson and Cowan rate equations, and provide tractable stochastic extensions of the purely deterministic standard neural-field models [12, 7]. The two approaches differ because they address two different regimes of network ac-

tivity: Buice, Cowan and Chow address the highly correlated Poisson-like activity and Paul Bressloff the asynchronous states. These different points of view lead the authors to define different variables and they obtain closely related yet different equations on the variables they define. They then derive equations for moments from the master equation which they then simplify and truncate to finite order.

The present paper is organized as follows: in the first section we describe the models we use. Both simplified models introduced involve coupling between mean firing rate and correlations between firing times, with finite-size correlations. In the second section, we are interested in the non-zero correlation solutions of the mean-field equations, and, in particular, focus on the qualitative similarities and differences between the solutions of these stochastic equations compared to the customary Wilson and Cowan behaviors. In the third section, we turn to study the finite-size effects, namely the qualitative differences between the solutions of mean-field limits and Wilson and Cowan system on one hand, and the behaviors of large but finite networks on the other hand. These finite-size solutions are compared back to the initial Markovian model and the differential equations they produced.

**1. Markovian firing models.** In this section, we introduce and describe the master equation formalism used by Buice and Cowan [12] (hereafter BCC) and Bressloff [7] and derived from [16], and extend these approaches to take into account different populations. Both models have been previously derived, so we quickly present here their derivation and the resulting equations in this section, as our main purpose is to study their solutions. More details on the derivation of these equations is provided in appendix A.

We consider a network structured into  $M$  homogeneous neural populations. Each population  $i \in \{1, \dots, M\}$  is composed of  $N_i$  neurons, and the total number of neurons is denoted by  $N$  (i.e.  $N = \sum_{i=1}^M N_i$ ). We are interested in the behavior of the network when the number of neurons  $N$  tends to infinity. In this limit, we assume that the proportion of neurons belonging to each population are non-trivial, i.e.  $\lim_{N \rightarrow \infty} N_i/N = \lambda_i \in (0, 1)$ . Each neuron of population  $i$  interacts with all the neurons of the network, with an efficiency denoted  $W_{ij}$ . These weights are assumed to scale as  $1/N_j$ , so that a given activity at the level of population  $i$  will produce a bounded activity at the level of population  $j$ . We therefore define the effective interconnection weights  $w_{ij}$  such that  $W_{ij} = w_{ij}/N_j$ . Each population is assumed to receive an input firing rate  $I_i(t)$  that will be assumed to be deterministic and constant for the rest of this paper.

**1.1. Deterministic Wilson and Cowan equations.** The Wilson and Cowan (WC) model is based on the assumption that the synaptic input current to each population is a function of the firing-rate of the pre-synaptic population, and that the contributions of the different populations are linearly summed to produce the post-synaptic population firing rate. It assumes moreover that the population-averaged firing rates  $\nu_i(t)$  are deterministic function of time that are governed by the equations:

$$\frac{d\nu_i(t)}{dt} = -\alpha_i \nu_i(t) + f_i \left( \sum_{j=1}^M w_{ij} \nu_j + I_i(t) \right) \quad (1.1)$$

where  $f_i$  is a function transforming an incoming current into an output firing rate and typically has a sigmoidal shape.  $\alpha_i$  are the relaxation rates corresponding to the natural inactivation of each population when they receive no input.

This purely deterministic approach, often used for spatially extended neural networks, has proved efficient to model certain phenomena, but fails to reproduce the stochastic behaviors that can appear at the level of population activity. We now introduce a stochastic framework that extends this framework in order to take into account the stochastic nature of the firing.

**1.2. Markovian Framework.** In the Markovian approach yielding the models considered in the paper, each neuron can be either quiescent or active (active meaning in the process of firing an action potential), and the state of the network is then described by the variable  $n \in \mathbb{N}^M$  where  $n_i(t)$  is the total number of active neurons in population  $i$ . This chain is modelled as a one-step discrete-time Markov process, i.e. the only possible transitions of this chain are assumed to be  $n_i \rightarrow n_i \pm 1$  for  $i \in \{1, \dots, M\}$ . Each active neuron of population  $i$  returns to a quiescent state with constant probabilistic rate  $\alpha_i$  and each quiescent neuron become active with a state-dependent rate  $F_i(n)$  depending on the inputs the neuron receives. The probability of the network to be in a state  $n$  at time  $t$  therefore satisfies a differential equation called the *master equation*:

$$\frac{dP(n, t)}{dt} = \sum_{i=1}^M \left[ \alpha_i (n_i + 1) P(n_{i+}, t) - \alpha_i n_i P(n, t) \right. \\ \left. + F_i(n_{i-}) P(n_{i-}, t) - F_i(n) P(n, t) \right]$$

A more detailed description of the model is provided in the appendix A. From this equation we can derive the moments of the Markov chain. In the present paper we adapt the BCC and Bressloff approaches to consider the rescaled mean firing rate defined as the instantaneous averaged proportion of active neurons in each population  $\nu_i(t) = \langle n_i(t) \rangle / N_i$ , and rescaled correlations as the average value of the correlations of the proportion of active neurons in each population  $C_{ij} = \langle n_i(t) n_j(t) \rangle / N_i N_j$ .

The equations for the moments involve averaged values of  $\langle F_i(n) \rangle$  which, since the activation is not affine, involve all the moments of the variable  $n$ , and therefore need to be truncated in order to obtain a closed set of equations. The choice of the function  $F_i$  is so far unspecified and will be defined in order to recover the WC equations in the mean-field uncorrelated limit.

With the aim of specifically investigating (uncorrelated) asynchronous states, Bressloff truncates the series expansion up to second order, and considers the evolution of two coupled variables: the mean firing-rate  $\nu_i$  and the correlation of the firing activity. After Taylor expansion and a Van-Kampen system-size expansion (see appendix A for more details), a specific choice of the activation function  $F_i$  is made so that one ends up with the following set of ordinary differential equations:

$$\begin{cases} \frac{d\nu_i}{dt} &= -\alpha_i \nu_i + f_i(s_i) + \frac{1}{2} f_i''(s_i) \sum_{k,l} w_{ik} w_{il} C_{kl} \\ \frac{dC_{ij}}{dt} &= \frac{1}{N_i} [\alpha_i \nu_i + f_i(s_i)] \delta_{i,j} - (\alpha_i + \alpha_j) C_{ij} \\ &+ \sum_k [f_i'(s_i) w_{ik} C_{kj} + f_j'(s_j) w_{jk} C_{ki}] \end{cases} \quad (1.2)$$

where we denote by  $s_i(t)$  the total instantaneous current received by population  $i$  at time  $t$ :

$$s_i(t) = \sum_{j=1}^M w_{ij} \nu_j(t) + I_i(t). \quad (1.3)$$

Buice and Cowan, interested in studying the Poisson-like firing modes of the network, transform the moment equations to derive equations of *normal ordered cumulants* measuring the deviations of the moments of the variable  $n$  from pure Poisson statistics. The first normal ordered cumulant is equal to  $\langle n_i \rangle$ , the second ordered cumulant to  $c_{ij} = C_{ij} - \nu_i/N_i\delta_{ij}$ . In terms of these variables after some approximations and moment truncation to the second-ordered cumulant, they end up with the following set of ordinary differential equations (this step involves an instantiation of the activation functions  $F_i$  different from the Bressloff case):

$$\begin{cases} \frac{d\nu_i}{dt} &= -\alpha_i\nu_i + f_i(s_i) + \frac{1}{2}f_i''(s_i)\sum_{j,k}w_{ij}w_{ik}c_{jk} \\ \frac{dc_{ij}}{dt} &= -(\alpha_i + \alpha_j)c_{ij} + f_i'(s_i)\sum_k w_{ik}c_{kj} + f_j'(s_j)\sum_k w_{jk}c_{ki} + \\ &+ \frac{1}{N_j}f_i'(s_i)w_{ij}\nu_j + \frac{1}{N_i}f_j'(s_j)w_{ji}\nu_i \end{cases} \quad (1.4)$$

We show in appendix A that these two models are indeed equivalent up to a change of variables and after truncation of the new equations. We now show that in the limit  $N \rightarrow \infty$ , both models converge to the same equations, called the *infinite-size system*, that we now introduce and study.

**1.3. The infinite-size model.** The microscopic model yielding BCC and Bressloff equations is exactly the same, and the two approaches yield similar equations as is apparent by comparing equations (1.4) and (1.2). The main differences are linked with the choice of phenomenon they want to account for, which yield different choice of variables and activation functions.

Interestingly, in the rescaled models we introduced, we observe that when the number of neurons tend to infinity, both Bressloff (1.2) and BCC (1.4) models converge to the same equations. These equations will be referred to as the *infinite size model* and are given by the equations:

$$\begin{cases} \frac{d\nu_i}{dt} &= -\alpha_i\nu_i + f_i(s_i) + \frac{1}{2}f_i''(s_i)\sum_{k,l}w_{ik}w_{il}\Delta_{kl} \\ \frac{d\Delta_{ij}}{dt} &= -(\alpha_i + \alpha_j)\Delta_{ij} \\ &+ \sum_k [f_i'(s_i)w_{ik}\Delta_{kj} + f_j'(s_j)w_{jk}\Delta_{ki}] \end{cases} \quad (1.5)$$

We recall that the interpretation of the variable  $\Delta$  generally varies: in BCC model  $\Delta_{ij} = c_{ij}$  are the second ordered cumulant, while in Bressloff model  $\Delta_{ij} = C_{ij}$  is the correlation in the firing activity. However, in the infinite-size limit, the normal ordered cumulant is equal to the correlations, and therefore  $\Delta_{ij}$  always corresponds to the correlations. However, when  $N$  becomes finite, the reader needs to bear in mind that in the finite-size unfolding of the infinite-size equations in BCC case,  $\Delta$  represents the deviation of spike statistics from a Poisson Process and in Bressloff model the covariance of the firing activity. When letting  $N$  be finite, the two models unfold the behavior of the system in a different fashion. We also note that if the variable  $\Delta(t)$  is equal to zero, then the mean-firing rates  $\nu_i(t)$  satisfy the WC equations. In that view, Bressloff and BCC models are generalizations of WC system that take into account the correlations in the firing.

In this paper, we will first be interested in studying the mean-field limit solutions of the infinite size equations (1.5), and second in unfolding these mean-field behaviors when the number of neurons is large but finite. Our study will particularly focus on two main aspects: (i) how the stochastic nature of the firings affect the observed behaviors at the macroscopic level through the interplay of firing activity and the correlations, and (ii) how the finiteness of the number of neurons in the network disturbs

these behaviors, and in particular, do WC equations or the infinite-size equations accurately approximate the behaviors of large networks.

Besides these theoretical analysis on the equations, we will also go back to the initial Markovian model and compare the stochastic behaviors it presents to the solutions of WC, BCC and Bressloff models.

**2. Influence of the correlations in the mean-field limit.** We have shown that in the limit where number of neurons is infinite, both Bressloff and BCC models converge to the infinite-size model given by equations (1.5) where the mean-firing rate is coupled to the correlations in the firing activity. When the correlations are equal to zero, the equation for the mean-firing rate is uncoupled from the one for the correlations  $\Delta$  and is identical to the WC system. The question we address in this section is how the interaction between the mean activity and the correlations modifies the behavior of the global activity compared to WC system given by equations (1.1). We address the following two questions: (i) are the solutions of Wilson and Cowan equations also solutions of the full systems including correlatons, and if the answer is yes, are the stability properties of these solutions conserved? and (2) Do the correlations yield other behaviors?

**2.1. Wilson and Cowan's Solution Solve the Infinite-Size System.** In equation (1.5), it is easy to see that zero correlation:  $\Delta(t) = 0$  is always a fixed point of the correlation equations no matter what mean firing rates  $\nu(t)$  are. For zero correlations, the equations for the mean firing rate  $\nu$  are reduced to the classical WC equations. Therefore, WC solutions define solutions for the infinite-size system with zero correlations. Let us now study the stability of the solutions defined by these uncorrelated WC behaviors in the infinite size system.

The infinite-size system involves a standard  $M$ -dimensional differential equation on the mean firing rates  $\nu(t)$  coupled to a matrix differential equation. In order to use customary approaches for dynamical systems, we transform the correlation matrix into a  $M^2$  dimensional vector and express the equations on  $\Delta$  in this new format using Kronecker products from linear algebra. To this end, we start by defining the function *Vect* transforming a  $M \times M$  matrix into a  $M^2$ -dimensional column vector, as defined in [29]:

$$Vect : \begin{cases} \mathbb{R}^{M \times M} & \mapsto \mathbb{R}^{M^2} \\ X & \mapsto [X_{11}, \dots, X_{M1}, X_{12}(t), \dots, X_{M2}(t), \dots, X_{1M}(t), \dots, X_{MM}(t)]^T \end{cases}$$

Let us now denote by  $\otimes$  the Kronecker product defined for  $A \in \mathbb{R}^{m \times n}$  and  $B \in \mathbb{R}^{r \times s}$  as the  $(mr) \times (ns)$  matrix:

$$A \otimes B := \begin{pmatrix} a_{11}B & a_{12}B & \cdots & a_{1n}B \\ a_{21}B & a_{22}B & \cdots & a_{2n}B \\ \vdots & \vdots & \ddots & \vdots \\ a_{m1}B & a_{m2}B & \cdots & a_{mn}B \end{pmatrix}$$

Some definitions and identities in the field of Kronecker products are reviewed in appendix B, and a more complete discussion can be found in [8] and references therein. We recall here for the sake of completeness some well-known relationship that will be useful. Let  $A, B, D, G, X \in \mathbb{R}^{M \times M}$ , let  $I_M$  be the  $M \times M$  identity matrix and  $A \cdot B$

or  $AB$  denote the standard matrix product. We have:

$$\begin{cases} \text{Vect}(AXB) = (B^T \otimes A)\text{Vect}(X) \\ A \oplus A = A \otimes I_M + I_M \otimes A \\ (A \otimes B) \cdot (D \otimes G) = (A \cdot D) \times (B \cdot G) \end{cases} \quad (2.1)$$

The relationship  $\oplus$  is called Kronecker sum. In this framework, we have the following identity:

LEMMA 2.1. *Let  $V_\Delta(t) = \text{Vect}(\Delta(t))$  be the column vectorization of the matrix  $\Delta(t)$ , and  $A(x)$  the matrix defined by  $A(x) = -\alpha + \mathbf{F}(x)$  where  $\alpha$  is the diagonal matrix with  $(i, i)$  element  $\alpha_{ii} = \alpha_i$  and  $\mathbf{F}$  the matrix of general element  $(\mathbf{F})_{ij} = (f'_i(\sum_{k=1}^M w_{ik} x_k)w_{ij})$ .*

*The variable  $V_\Delta(t)$  satisfies the differential equation in  $\mathbb{R}^{M^2}$ :*

$$\frac{dV_\Delta(t)}{dt} = (A(\nu(t)) \oplus A(\nu(t)))V_\Delta(t). \quad (2.2)$$

*Proof.* The differential equation governing the evolution of the coefficients of the correlation matrix  $\Delta(t)$  of the infinite size system (1.5) can be easily reordered into:

$$\frac{d\Delta_{ij}}{dt} = \sum_{k=1}^M (A_{ik}(\nu(t))\Delta_{kj}(t) + A_{jk}(\nu(t))\Delta_{ik}(t))$$

which, through straightforward linear algebra manipulations, can be written as:

$$\frac{d\Delta}{dt} = A(\nu(t)) \cdot \Delta(t) + \Delta(t) \cdot A(\nu(t))^T.$$

The linear operator  $X \mapsto A(\nu(t)) \cdot X + X \cdot A(\nu(t))^T$  for  $X \in \mathbb{R}^{M \times M}$  can be written in terms of Kronecker product of matrix on the vectorized version  $V_\Delta(t)$  of the matrix  $\Delta(t)$  using the relationship given in (2.1) and we have:

$$\begin{aligned} \text{Vect}(A(\nu(t)) \cdot \Delta(t) + \Delta(t) \cdot A(\nu(t))^T) &= \text{Vect}\left(A(\nu(t)) \cdot \Delta(t) \cdot I_M\right) + \text{Vect}\left(I_M \cdot \Delta(t) \cdot A(\nu(t))^T\right) \\ &= \left(I_M^T \otimes A(\nu(t)) + A(\nu(t)) \otimes I_M\right) \cdot V_\Delta(t) \\ &= \left(A(\nu(t)) \oplus A(\nu(t))\right) \cdot V_\Delta(t). \end{aligned}$$

□

Now that we have defined a convenient framework to study the infinite size equations, we are in position to study the stability of fixed points and limit cycles of the WC system as solutions with zero correlations of the infinite size system. We start by addressing the problem in the one population model ( $M = 1$ ), which allows straightforward calculations and will be helpful in our specific study of the one population infinite-size equation.

PROPOSITION 2.2. *In the one population case, any fixed point of Wilson and Cowan equation is a zero-correlation fixed point of the infinite-size system, and with the same stability properties.*

*Proof.* In the one population case, equations (1.4) constitute a planar dynamical system that reads:

$$\begin{cases} \frac{d\nu}{dt} = -\alpha\nu + f(s) + \frac{1}{2}f''(s)w^2\Delta \\ \frac{d\Delta}{dt} = -2\alpha\Delta + 2f'(s)w\Delta \end{cases} \quad (2.3)$$

where  $s = w\nu + I$ .

As stated, the solution  $\Delta = 0$  is a fixed point of the correlation equation, and in that case, the activity satisfies the one-population WC equation:

$$\frac{d\nu}{dt} = -\alpha\nu + f(w\nu + I)$$

Let  $\nu^*$  be a fixed point of this system. The Jacobian matrix of the infinite-size system at the fixed point  $(\nu^*, \Delta \equiv 0)$  reads:

$$\begin{pmatrix} -\alpha + w f'(w\nu^* + I) & \frac{1}{2} f''(w\nu^* + I) w^2 \\ 0 & 2(-\alpha + w f'(w\nu^* + I)) \end{pmatrix}$$

As we can obviously see, the eigenvalues of this equilibrium are  $\lambda_1 := (-\alpha + w f'(w\nu^* + I))$  and  $\lambda_2 = 2\lambda_1$ , and therefore the stability of this fixed point is the same as the stability of the related fixed point in WC's system.  $\square$

We therefore conclude that any stable solution of the one dimensional WC equation provides a zero correlation ( $\Delta = 0$ ) stable fixed point of the infinite-size system, and we observe that no stable solution of WC system is destabilized by the presence of correlations, and no unstable solution of the Wilson and Cowan equation will be stabilized. Therefore, zero-correlation fixed points of the infinite size system exists if and only if Wilson and Cowan equation has a fixed point, and the related fixed point of the infinite-size system has the same stability as WC's fixed point.

We now turn to demonstrating the related properties in arbitrary dimensions  $M$ , for fixed points and cycles.

**THEOREM 2.3.** *Solutions of the WC system provide solutions of the infinite-size system with zero correlations  $\Delta = 0$ . The stability of fixed points and limit cycles of the infinite size system depend on the stability of the solution for the WC system as follows:*

*i) A fixed point of the infinite-size equation with null correlations is stable if and only if the value of related mean-firing rate is a stable fixed point of WC system;*

*ii) A cycle of the infinite size system with zero correlations  $(\nu(t), \Delta \equiv 0)$  is exponentially unstable if and only if  $\nu(t)$  is an unstable cycle of WC system. Stable cycles  $\nu(t)$  of WC's system define cycles of the infinite-size system with zero correlations with neutral linear stability. The infinite size system does not present any stable cycle with null correlations.*

*Proof.* In order to prove the theorem, it is convenient to introduce the vector fields  $F_\nu : \mathbb{R}^M \mapsto \mathbb{R}^M$ ,  $G_\nu(\nu) : \mathbb{R}^M \mapsto \mathbb{R}^{M \times M^2}$  and  $F_\Delta : \mathbb{R}^M \mapsto \mathbb{R}^{M^2 \times M^2}$  that govern the dynamics of the infinite size system:

$$\begin{cases} \frac{d\nu}{dt} &= F_\nu(\nu) + G_\nu(\nu)V_\Delta(t) \\ \frac{dV_\Delta}{dt} &= F_\Delta(\nu)V_\Delta(t) \end{cases}$$

We have  $F_\nu(\nu) = -\alpha + [f_i(s_i), i = 1 \dots M]^T$ ,  $F_\Delta(\nu) = A(\nu) \oplus A(\nu)$  where  $A(\cdot)$  is defined in lemma 2.1, and  $G_\nu(\nu)$  is the  $M^2 \times M^2$  matrix such that:

$$G_\nu(\nu)V_\Delta(t) = \left[ \frac{1}{2} f''_i(s_i) \sum_{k,l} w_{ik} w_{il} \Delta_{kl}, i = 1 \dots M \right]^T$$

Let  $(\nu(t), \Delta \equiv 0)$  be a solution of the infinite-size system. The Jacobian matrix of the system evaluated on this solution has the form:

$$\begin{aligned} J(\nu(t), 0) &= \begin{pmatrix} d_\nu(F_\nu) + d_\nu(G_\nu)V_\Delta \Big|_{\nu(t), V_\Delta \equiv 0} & G_\nu(\nu) \Big|_{\nu(t), V_\Delta \equiv 0} \\ d_\nu(F_\Delta)V_\Delta \Big|_{\nu(t), V_\Delta \equiv 0} & d_{V_\Delta}(F_\Delta) \Big|_{\nu(t), V_\Delta \equiv 0} \end{pmatrix} \\ &= \begin{pmatrix} d_\nu(F_\nu)(\nu(t)) & G_\nu(\nu(t)) \\ \mathbf{0} & d_{V_\Delta}(F_\Delta)(\nu(t)) \end{pmatrix} \end{aligned}$$

where  $d_X f$  for a multidimensional vector  $X$  and a multidimensional function  $f$  denotes the differential of  $f$  with respect to  $X$ . Since  $F_\nu$  is exactly the vector field associated with WC system,  $d_\nu F_\nu$  is an  $M \times M$  block corresponding to Jacobian matrix of WC system at the point  $\nu$ , which is equal to the matrix  $A(\nu)$  introduced in lemma 2.1.

Now that the Jacobian matrix is identified, we prove the assertions of the theorem:

*i)* Let us consider a fixed point  $(\nu, \Delta \equiv 0)$  of the infinite size system. Necessarily,  $\nu$  is a fixed point of Wilson and Cowan equation. The stability of this fixed point depends on the spectrum of the Jacobian matrix  $J$  of the system at this point. Since the Jacobian matrix of the infinite-size system is block diagonal, its spectrum is therefore composed of the eigenvalues each diagonal block  $d_\nu(F_\nu) = A(\nu)$  and  $d_{V_\Delta}(F_\Delta)(\nu(t))$ . The first block,  $A(\nu)$ , has exactly the eigenvalues of Wilson and Cowan system at its fixed point  $\nu$ . These eigenvalues are denoted  $\{\lambda_i, i = 1 \dots M\}$ . The second diagonal block of the Jacobian matrix  $d_{V_\Delta}(F_\Delta)$  is equal to the Kronecker sum  $A(\nu) \oplus A(\nu)$  as a simple corollary of lemma 2.1. The eigenvalues of a Kronecker sum are known to be all possible pairwise sums of all the eigenvalues of  $A(\nu)$ , viz.  $(\lambda_i + \lambda_j; (i, j) \in \{1, \dots, M\}^2)$  (see an elementary proof of this fact in proposition B.1 of appendix B), hence the spectrum of the Jacobian matrix of the infinite size system is composed of the eigenvalues:

$$\{\lambda_i, i = 1 \dots M\} \cup \{\lambda_i + \lambda_j, (i, j) \in \{1, \dots, M\}^2\}.$$

These eigenvalues depend in a simple fashion on the eigenvalues of the WC Jacobian matrix at the fixed point  $\nu$ , and it is easy to show that the fixed point  $(\nu, 0)$  in the the infinite system is:

- exponentially stable if and only if the  $\nu$  is an exponentially stable fixed point of WC system, i.e. if and only if all the eigenvalues  $\lambda_i$  have a strictly negative real part.
- exponentially unstable if and only if the  $\nu$  is an exponentially unstable fixed point of WC system, i.e. if and only if there exists an eigenvalue  $\lambda_i$  with strictly positive real part.
- neutrally stable if and only if  $\nu$  is neutrally stable for WC system, i.e. if and only if all eigenvalues have non-positive real part and at least one eigenvalue have a null real part.

In summary, the stability of the zero-correlation fixed point  $(\nu, \Delta \equiv 0)$  is exactly the same as the stability of  $\nu$  as a fixed point of WC system.

*ii)* Let us now address the case of cycles with null correlations. To this end, let us consider that  $(\nu(t), \Delta(t) \equiv 0)$  is a periodic orbit of the infinite-size system ( which entails  $\nu(t)$  is a periodic orbit of a WC system). Let us denote by  $T > 0$  the period of this cycle. We show that the null correlations  $\Delta \equiv 0$  is an exponentially unstable

solution if the cycle  $\nu(t)$  is exponentially unstable as a solution of WC system, and neutrally stable if the cycle  $\nu(t)$  is exponentially stable or neutrally stable as a solution of Wilson and Cowan system, which entails the proof of the theorem.

Given that the cycle  $\nu(t)$  is known, the correlations  $\Delta(t)$  satisfy a linear equation:

$$\frac{dV_{\Delta}(t)}{dt} = \left( A(\nu(t)) \oplus A(\nu(t)) \right) V_{\Delta}(t)$$

and the time-dependent matrix  $\left( A(\nu(t)) \oplus A(\nu(t)) \right)$  is  $T$ -periodic. A basic result of Floquet theory implies that the stability of the solution  $V_{\Delta} \equiv 0$  depends on the eigenvalues of the resolvent of the system at time  $T$ , namely the matrix  $\Psi(T)$  in  $\mathbb{R}^{M^2 \times M^2}$  where  $\Psi(\cdot)$  is defined by

$$\begin{cases} \frac{d\Psi(t)}{dt} &= \left( A(\nu(t)) \oplus A(\nu(t)) \right) \Psi(t) \\ \Psi(0) &= I_{M^2} \end{cases}$$

More precisely, the null fixed point is exponentially stable if and only if all eigenvalues of  $\Psi(T)$  ( the *multipliers* ) are of modulus strictly smaller than 1, neutrally stable if all have modulus smaller or than equal to 1 with at least one multiplier with modulus equal to 1, and exponentially unstable if there exists a multiplier with modulus larger than 1. We therefore need to characterize the eigenvalues of  $\Psi(T)$  in order to conclude on the stability of the solution in the infinite-size system. To this end, let us introduce  $\Phi(t)$  the resolvent of WC system, i.e. the unique solution of the fundamental equation:

$$\begin{cases} \frac{d\Phi(t)}{dt} &= A(\nu(t))\Phi(t) \\ \Phi(0) &= I_M \end{cases}$$

We prove in theorem B.2 of appendix B that  $\Psi(t) = \Phi(t) \otimes \Phi(t)$ . Let us denote by  $\{\mu_i, i = 1, \dots, M\}$  the eigenvalues of  $\Phi(T)$ . Because  $\Psi(T)$  is the Kronecker square of  $\Phi(T)$ , its eigenvalues are all pairwise products of the eigenvalues of  $\Phi(T)$ , viz.  $\{\mu_i \mu_j, i, j = 1 \dots M\}$ , as shown in proposition B.1 of appendix B.

If the cycle  $\nu(t)$  is exponentially unstable as a solution of WC system, then Floquet theory implies that there necessarily exists a multiplier of  $\Phi(T)$ ,  $\mu_i$ , such that  $|\mu_i| > 1$ . Therefore the resolvent  $\Psi(T)$  has a multiplier equal to  $\mu_i^2$  which has modulus equal to  $|\mu_i|^2 > 1$  and therefore this cycle is exponentially unstable as a solution of the infinite-size system.

If  $\nu(t)$  is exponentially stable or neutrally stable as a solution of WC system, then a basic result of Floquet theory states that the resolvent if the linearized system evaluated on the cycle at time  $T$ , namely  $\Phi(T)$ , has at least a multiplier equal to 1 and all other multipliers with multipliers of modulus smaller than 1. We now provide an elementary proof of the existence of the 1 multiplier: let  $\xi(t) = F_{\nu}(\nu(t))$ . Then since  $\nu(t)$  is  $T$ -periodic, so is  $\xi(t)$ , and furthermore we have:

$$\frac{d\xi(t)}{dt} = \frac{dF_{\nu}(\nu(t))}{dt} = (d_{\nu}F_{\nu})(\nu(t)) \frac{d\nu(t)}{dt} = (d_{\nu}F_{\nu})(\nu(t)) F_{\nu}(\nu(t)) = A(\nu(t)) \xi(t)$$

Moreover, since  $\nu(t)$  is not a fixed point,  $F(\nu(0)) \neq 0$ . We have shown  $\xi(t)$  is solution of the linearized equation and hence using its  $T$ -periodicity, we have  $\xi(T) = \Phi(T)\xi(0) = \xi(0)$ , which proves that  $\xi(0)$  is eigenvector of  $\Phi(T)$  associated with the eigenvalue 1. Therefore, the resolvent  $\Psi(T)$  necessarily has an eigenvalue equal to

one (associated with the eigenvector  $\text{Vect}(\xi(0)\xi(0)^T)$ ), which implies that the null fixed point has a neutral linear stability as a solution of the infinite-size system. We directly conclude from this result that the infinite size system does not features any exponentially stable cycle, which ends the proof.  $\square$

We conclude that the solutions of WC system always provide solutions of the infinite-size system, and that all fixed points with null correlations in the infinite-size system are fixed points of WC system, with the same stability properties. However, cycles of WC system lose exponential stability in the infinite-size system. Note that this does not necessarily implies that these cycles become unstable, and a nonlinear stability analysis is necessary. But it implies that the transient phase of convergence towards the cycle or of repulsion from the cycle will be not be exponential. This qualitative difference suggests a way to distinguish the two models and validate the choice of the one or the other model.

**2.2. Correlation-induced behaviors.** In the previous section, we just proved that all the fixed points of the WC system are solutions of uncorrelated activity in the infinite size system. We now investigate the existence of new solutions induced by the presence of non-null correlations in the infinite system, that are therefore not solutions of WC system. Such solutions will be referred to as *correlation-induced behaviors*. The general resolution of this problem is quite hard in the general case. For this reason, we provide a rigorous analysis of the one population case, and treat two-population case through numerical analysis and simulations.

**2.2.1. One population case.** We have seen in the one population case that any fixed point of WC system was solution of the infinite size system with zero correlations. Moreover, there is no possible cycle in Wilson and Cowan equations in one dimension. We investigate now the existence of cycles or additional fixed points in the infinite size system with one population. We recall that acceptable solutions in the one population case necessarily have non-negative firing rate  $\nu$  and  $\Delta$ . Indeed, in the case of the infinite-size model arising in the limit of Bressloff's rescaled model, the correlation  $\Delta$  needs to be positive as a limit of positive quantities (and as the covariance of the Markov process), and in BCC case  $\Delta$  is equal to the correlation up to the coefficient  $-\nu/N$  that vanishes in the infinite-size limit.

**THEOREM 2.4.** *In the one population infinite size system, there does not exist any acceptable stable fixed point with strictly positive correlation  $\Delta$ .*

*Proof.* Let us assume that  $\Delta \neq 0$ . The fixed point equation of the infinite-size system:

$$\begin{cases} -\alpha + f'(w\nu + I)w = 0 \\ -\alpha\nu + f(w\nu + I) + \frac{1}{2}f''(w\nu + I)w^2 \Delta = 0 \end{cases} \quad (2.4)$$

The first equation of the system (2.4) is independent of  $\Delta$  and fixes possible values of  $\nu$ . Assuming that this equation has a solution  $\nu^*$  and denoting  $s^* = w\nu^* + I$ , the Jacobian matrix of the system at  $\nu = \nu^*$  reads, using the property that  $\nu^*$  solves the first equation of (2.4):

$$\begin{pmatrix} \frac{1}{2}f'''(s^*)w^3\Delta & \frac{1}{2}f''(s^*)w^2 \\ 2f''(s^*)w^2\Delta & 0 \end{pmatrix} \quad (2.5)$$

Such values of  $\nu^*$  necessarily exist for some parameters, and since the function  $f$  is assumed to be sigmoidal, it can have multiple solutions. Moreover, because of the

particular shape of the sigmoidal function  $f$ , the second derivative of  $f$  can vanish at a point corresponding to the inflection point of the sigmoid.

In a very particular case (for precisely tuned values of the parameters), one can hence have  $f''(w\nu^* + I) = 0$ . In that case, fixed points only exist if  $-\alpha + f'(w\nu^* + I)w = 0$ , if this condition is satisfied, any value of the correlation  $\Delta$  provides a fixed point of the system. This fixed point is never exponentially stable, since in that case the Jacobian matrix has a zero eigenvalue (obvious when using the expression of the Jacobian matrix (2.5) and using the fact that  $f''(s^*) = 0$ ).

In the general case where  $f''(s^*) \neq 0$ , the system has a fixed point with non-null correlations

$$\left( \nu^*, \Delta^* := 2 \frac{\alpha\nu^* - f(s^*)}{w^2 f''(s^*)} \right).$$

We therefore need to check whether if this fixed point is stable and acceptable (i.e.  $\min(\nu^*, \Delta^*) \geq 0$ ). The Jacobian matrix at this point has the expression given by (2.5). Its determinant is equal to  $-(f''(s^*))^2 w^4 \Delta^*$  and has an opposite sign than  $\Delta^*$ . Therefore, for acceptable solutions with  $\Delta^* > 0$ , the determinant of the Jacobian matrix is strictly negative. We conclude that any fixed point of the infinite-size system with  $\Delta > 0$  are saddle fixed points.  $\square$

We conclude from this theorem that the system does not features any acceptable stable fixed point with non-zero correlations.

Let us now address the existence of acceptable cycles in the system. First of all, we show that the system does not feature any generic bifurcation that can yield cycles. It is easy to show that for input current  $I$  very large the system only has a unique fixed point with zero correlation, with mean firing rate  $\nu$  corresponding to the fixed point of WC system. Indeed, the fixed point equation on the correlations reads:

$$(-\alpha + f'(w\nu + I)w) \Delta = 0.$$

Because of the properties of the sigmoidal function  $f$ , we have that for  $I$  sufficiently large,  $-\alpha + f'(w\nu + I) < 0$  for any acceptable  $\nu \geq 0$ . Therefore the only acceptable solution of this equation is  $\Delta = 0$ , corresponding to the WC system, that does not present any bifurcation that can possibly yield to oscillations. The only possible bifurcations along this point are degenerate, because of the form of the Jacobian matrix as exhibited in the proof of theorem 2.4, and therefore no cycle appear through bifurcation of this branch of fixed points. The new fixed points with non-zero correlations appear through a singular bifurcation when varying parameter  $\alpha$ . Indeed, for these fixed points to exist, there need to exist a solution to the equation  $-\alpha + f'(w\nu^* + I)w = 0$ , i.e.  $f(w\nu^* + I) = \alpha/w$ . The function  $f'$  is bounded, let us denote by  $A$  its maximal value. The fixed point with non-null correlation appear for  $\alpha^* = Aw$ . At the value of the critical parameter  $\alpha^*$ , the fixed point appears at where the function  $f'(w\nu + I)$  reaches its maximal value, and therefore  $f''(w\nu + I)$  vanishes. The fixed point therefore diverges close to the bifurcation<sup>1</sup>, and one cannot infer from this singular bifurcation any information on the presence of cycles. These fixed points are always saddles, hence there is no possible Hopf bifurcation and no cycle appears from this branch of fixed points. Therefore these methods establish that along the branches of fixed point, no cycle is generated through bifurcations. This does not imply that the system does not feature any periodic orbit at all, and we end the

<sup>1</sup>Moreover, the system does not satisfies the genericity conditions as given in [23] or [24].

analysis of the system by performing an extensive exploration of the parameter space and initial conditions in search for periodic solutions, for a given choice of sigmoidal function set to be the classical sigmoid

$$f(x) = \frac{1}{1 + \exp(-x)}$$

Hopefully, since the system only features 3 parameters and 2 variables, the exploration is quite easily done, and no cycle was found, therefore no cycle exists in the range of parameters considered.

We conclude from this semi-analytical analysis that the only acceptable stable fixed points of the system are the one provided by WC system, and that the presence of correlations does not generate cycles. The only stationary states are therefore uncorrelated states with firing rates given by WC equations, and no periodic solution appears. This situation will be quite different in the multi-population case, as we now develop.

**2.2.2. Correlation-induced behaviors in multi-populations networks.** We now turn to study multi-population networks with the aim of identifying solutions of the infinite-size system that qualitatively differ from WC equation. The situation in the multidimensional case will be quite different, since we have proven in theorem 2.3 that cycles of WC system lost exponential stability in the infinite-size system, allowing the appearance of distinct transient and/or asymptotic behaviors.

To identify such correlation-induced behavior we numerically study two particular two population networks. The first model (Model I) is a two-population network including an excitatory and an inhibitory population known to produce oscillations, and the second example (Model II) builds on a famous model of binocular rivalry presenting bistability of fixed points.

*Perturbation of a WC cycle.* We proved in theorem 2.3 that any cycle of WC model lost exponential stability in the infinite-size system. This loss of exponential stability does not necessarily mean that the cycle loses stability, and this property depends on the higher order terms of the nonlinear equation, but even if the cycle keeps stability, the transient convergence phase towards the cycle will be dramatically slowed.

In this section, we choose to study a two-populations network featuring an excitatory population interconnected with an inhibitory one. To fix ideas, we denote by 1 (resp. 2) the excitatory (resp. inhibitory) populations. We choose the same activation function for both populations equal to  $f(x) = 1/(1 + \exp(-x))$  and the same inactivation rate  $\alpha = 1$ , and are interconnected through the following connectivity matrix:

$$\begin{pmatrix} w_{11} = 15 & w_{12} = -12 \\ w_{21} = 16 & w_{22} = -5 \end{pmatrix}.$$

Each population receives different input currents  $I_1 = -0.5$  and  $I_2 = -5$ . These parameters define a model called Model I in the sequel. For these functions and parameters, the WC system features a cycle. When taking the input to the excitatory population  $I_1$  small, the system features a single stable fixed point, that loses stability as the input  $I_1$  increases through a supercritical Hopf bifurcation generating a family of stable limit cycles, that vanish through a saddle-node homoclinic bifurcation (see Figure 2.1(a)), branching onto a high-state stable fixed point. Let us now analyze how this picture is modified by the presence of correlations.

First of all, from theorem 2.3, it is clear that the parameter point where WC system undergoes the supercritical Hopf bifurcation will be a very degenerate bifurcation point for the infinite-size system. Indeed, the Hopf bifurcation is characterized by the presence of a pair of purely imaginary complex conjugate eigenvalues. Then lemma 2.1 and the fact that the Kronecker sum of two matrixes has all pairwise sums of eigenvalues of the matrixes in the sum (see appendix B) directly implies that the Jacobian matrix of the full system (1.5) has the eigenvalues  $\{\pm\lambda, \pm 2\lambda, 0\}$  and the eigenvalue 0 is of multiplicity two. Therefore at this point, the Jacobian matrix of the infinite size system has its 6 eigenvalues having a null real part, and thus at this point the system is very degenerate and the bifurcation is not a generic Hopf bifurcation. It is quite difficult numerically and analytically to study the solutions emerging from this bifurcation point, and many solutions can appear at this point, including cycles and fixed points. Similarly, at the two saddle-node bifurcations of WC system, since the Jacobian matrix of the infinite-size system has all the pairwise sums of the eigenvalues, it will have two null eigenvalues and therefore a degenerate bifurcation. The behaviors will appear more clearly in the finite-size unfolding of these degenerate bifurcation points. We do not address here the problem of classifying all behaviors of the system, but rather address the question of whether the WC cycle keeps a nonlinear stability in the new system. To answer this question, we perturb WC's cycle by adding a small initial condition in the correlations. Interestingly, we observe that a new cycle appears, that is attractive in a certain range of parameters (see Figure 2.1). The WC cycle does not completely loses stability and still appears as the only behavior of the system in a certain range of input values (e.g.  $I_1 = -0.5$  as plotted in Figure 2.1(b)). But for smaller values of the parameters, it loses its nonlinear stability and the additional cycle appears (e.g.  $I_1 = -2$  and Figure 2.1(c) and (d)). This new cycle is totally different in its shape, has a period close to half the period of the cycle corresponding to WC system, and has non-zero correlations that vary periodically at the same frequency. A continuation of this branch of cycles shows that it is stable in a significant range of parameters (Figure 2.1(e)). It loses stability when  $I_2$  decreases through a period-doubling bifurcation, and as  $I_2$  increases through a Neimark-Sacker bifurcation. This branch of limit cycles emerges from the very degenerate point corresponding to the Hopf bifurcation of WC system, as we expected. It disappears at a point corresponding to a subcritical Hopf bifurcation with correlations (on a branch of unstable fixed points that is not plotted in the diagram but that will be further investigated in section 3.2).

We conclude with a further observation on transient behavior. We have seen that WC's cycle was neutrally stable, but in some regions of parameters, it has nonlinear stability. In the region of parameters where the WC cycle is nonlinearly stable (white region in figure 2.1(d)), the transient phase of convergence towards this cycle takes a long time. In the green region where it is nonlinearly unstable, the neutral stability of the cycle produce some very strange transient behaviors where the activity of the cortical column is trapped around the neutrally stable WC system for long times, before leaving the neighborhood of this solution and converging towards the only stable solution which is the new cycle.

*Correlation-induced oscillations.* Correlations can have even more dramatic effects than modifying a periodic orbit as shown in Model I, and in this section we describe a case where a periodic orbit arises for parameter values where Wilson and Cowan system only fixed-points. To this end, we choose a two-population network known to have bistability. This model consists of two-populations with inhibitory

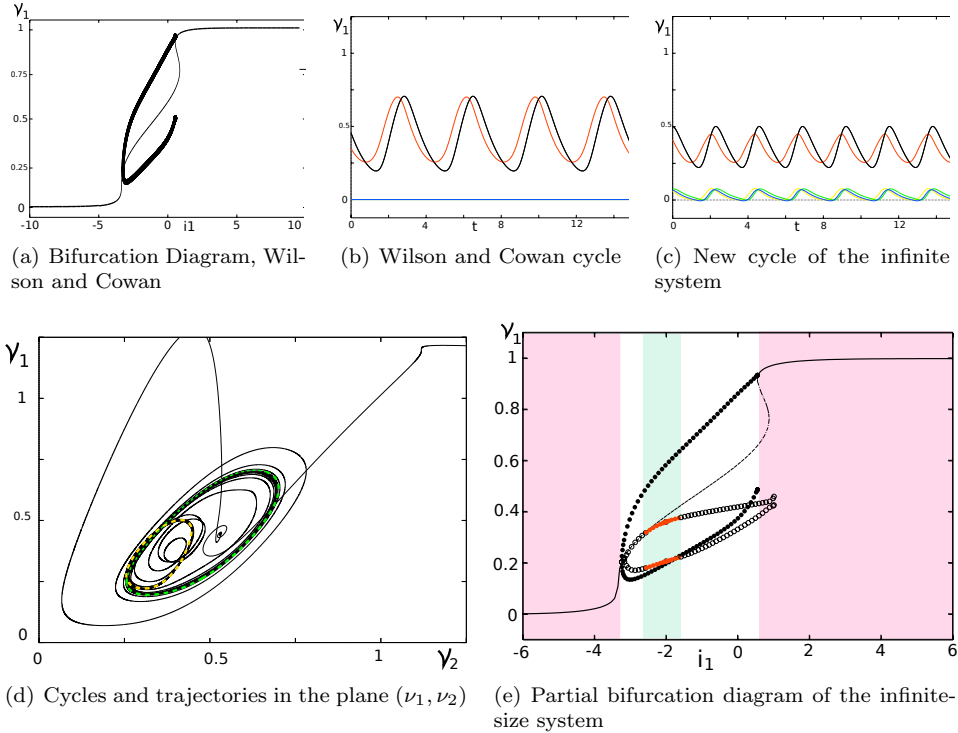


FIG. 2.1. *Model I: Comparison between WC system and the infinite-size system: (a) and (d) are the bifurcation diagram with respect to the parameter  $I_1$  of respectively WC and the infinite-size system. The thick lines represent stable fixed point, thin lines unstable fixed points, plain circles the extremal values of a stable cycle and empty circle unstable cycles. (b) represents WC cycle as a solution of the infinite-size system, which shows null correlations. red:  $\nu_1$ , white:  $\nu_2$ , yellow:  $\Delta_{11}$ , green:  $\Delta_{22}$ , blue:  $\Delta_{12} = \Delta_{21}$ . For non-zero correlations of the initial condition, the solution converges towards a new cycle with correlations (c) and (d) which is stable in a determined region of parameters.*

interactions and no self-interaction. The connectivity matrix in that case reads:

$$\begin{pmatrix} w_{11} = 0 & w_{12} = -12 \\ w_{21} = -12 & w_{22} = 0 \end{pmatrix}.$$

The inactivation constants  $\alpha_i$  are assumed constant equal to 1, and the inputs to the two populations are distinct and denoted  $I_1$  and  $I_2$ . The firing rate function are also identical and we make the usual choice  $f_i(x) = 1/(1 + \exp(-x))$  for  $i \in \{1, 2\}$ . These parameters define a model called Model II.

We break the symmetries between the two populations by considering that each population can receive different input, we freeze the input  $I_2$  and let  $I_1$  vary. In that case, the standard WC system presents a bistable behavior between two stable fixed points as we illustrate in Figure 2.2. The infinite size system driven by equations (1.5) with these parameters has much richer dynamics, as illustrated in Figure 2.2. We first set  $I_2 = 0$  and study the bifurcation diagram as  $I_1$  varies. We observe that the infinite-size system features a stable limit cycle, which is a qualitatively nontrivial effect of the correlations in the mean-field limit. All fixed-points behaviors in WC system are preserved, as predicted by theorem 2.3 (black curves in Figure 2.2(b)), but

new fixed points with non-zero correlations appear (blue lines in the diagram). Along one of the newly generated branch of fixed point, a supercritical Hopf bifurcation appears, generating a family of stable limit cycles (red circles in Fig. 2.2(b)) that further undergoes few consecutive period doubling bifurcations. We note that the new branch of fixed points intersects the branch of fixed points of Wilson and Cowan system precisely at the saddle-node bifurcations of Wilson and Cowan system. This fact is compatible with a partial result of the proof of theorem 2.3: at the saddle-node bifurcation, instead of a single eigenvalue equalling zero, two eigenvalues are simultaneously equal to zero, and the saddle-node bifurcations of WC system appear as transcritical bifurcations in the infinite size system. Note that in that case, the WC behavior is nowhere the unique stable behavior of the system, and for any value of the input parameter  $I_1$ , the infinite system will present attractive behaviors that are different from the WC behaviors. In particular, it has stable fixed points with non-zero correlations and non-zero correlation oscillations. However, we note that though these behaviors exist in the dynamics, the newly discovered fixed points do not constitute acceptable solutions since they are characterized by a negative firing-rate  $\nu_2$  and a non-positive definite correlation matrix. These behaviors, though present as solutions of the infinite-size system, will therefore not be displayed by any Markov model and are artificial. However, the cycles constitute acceptable solutions that could have counterparts in the Markov system.

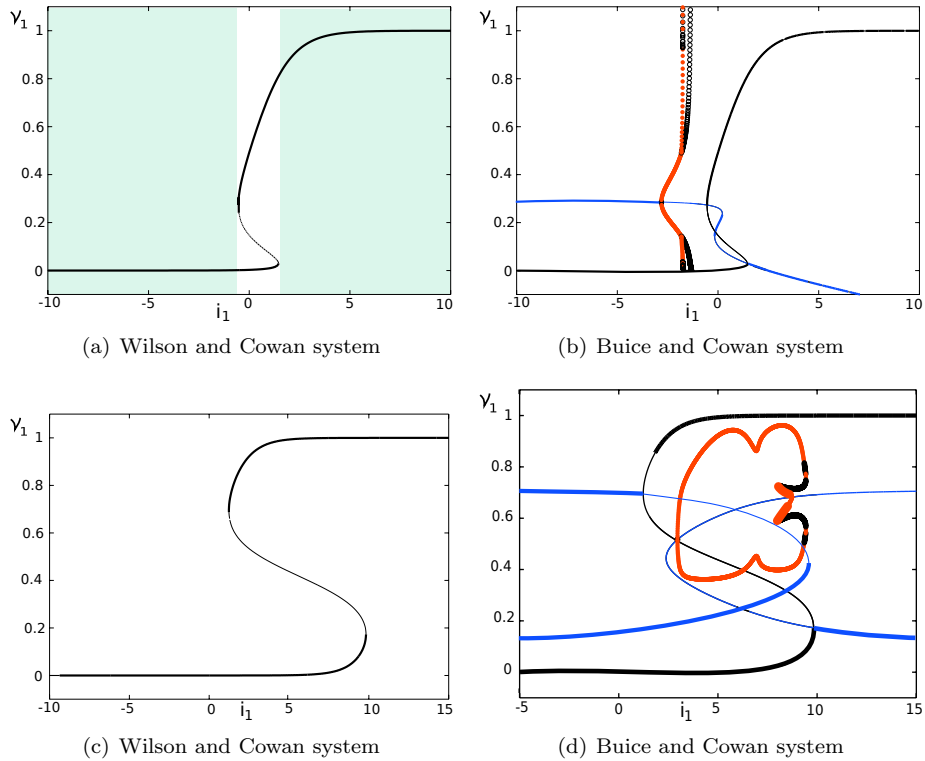


FIG. 2.2. Model II, Wilson and Cowan (left column) and infinite-size (right column) systems, with  $I_2 = 0$  (top row) and  $I_2 = 5$  (bottom row).

We further explore this model by choosing a large value of the input parameter

to the second population,  $I_2 = 5$ . For this level of input, the bifurcation diagram of WC system presents exactly the same features as in the case  $I_2 = 0$ , namely two saddle-node bifurcations and a region of bistability of fixed points. The infinite-size system, similarly to the case  $I_2 = 0$ , also has additional branches of fixed points with non-zero correlations that are connected to WC bifurcation diagram at the saddle-node bifurcation points. These saddle-nodes are degenerate and non-generic in the infinite size system from lemma 2.1 and become transcritical bifurcations. These additional non-zero correlation fixed points can be stable or unstable, depending on the parameter, and add additional possible behaviors. From one of these branches, the system undergoes a supercritical Hopf bifurcation and a family of stable limit cycles appears. This branch of limit cycles undergoes two period-doubling bifurcations, torus bifurcations and two fold of limit cycles, yielding additional oscillatory behaviors to the purely fixed-point structure of WC system.

From all these observations on both models, we conclude that the infinite-size system, besides featuring the same solutions as Wilson and Cowan system as a subset of solutions with zero correlations, also has additional behaviors that qualitatively differ from the Wilson and Cowan system. The mean-field limit including correlations is therefore a more complex system than WC system, in which correlations of the firing activity interact in a non-trivial way with the mean firing rate yielding complex behaviors. These qualitative correlation-induced behaviors can therefore be a good indicator of which model better accounts for the behavior of cortical columns and cortical areas.

We now turn to investigating finite-size effects arising from the finiteness of the number of neurons in a network.

**3. Finite-size effects.** The bifurcation diagram displayed by the infinite-size system studied in the previous section is composed of some very degenerate points, and displays behaviors the WC system does not display. The question that naturally arises at this point is to understand whether the infinite-size model or WC model really capture the qualitative behavior of large networks in the Markovian framework, and how these behaviors compare to BCC and Bressloff finite-size equations.

In this section we first study how the infinite-size bifurcation diagram is unfolded in finite-size networks, before simulating the Markov process and comparing its global behaviors to the behaviors of the finite-size systems. We observed that the finite-size BCC and Bressloff equations appeared as a perturbation of the infinite-size system, in which the size of the network appears as a parameter of the equations. In all of this study, instead of considering discrete population sizes, we will consider the inverse of the total population size  $n = 1/N$  as a continuous parameter. Non-trivial distinctions between finite-size networks and infinite size equation will essentially appear at the bifurcation points. Indeed, since both the rescaled Bressloff and BCC models vector fields are continuous with respect to the parameter  $n$ , when the infinite-size system ( $n = 0$ ) exhibits an hyperbolic fixed point, this fixed point will have a counterpart with the same stability for finite sufficiently large networks, by application of the implicit functions theorem. This is also the case of hyperbolic fixed points of WC system, since these are hyperbolic fixed points of the infinite-size system with zero correlations. In order to study common points and qualitative differences between finite-size networks and the infinite size limit, we will therefore focus on the bifurcations of both systems and numerically study the codimension two bifurcations in the one and two populations cases, with respect to the size of the network and to another parameter of interest (for instance an input parameter).

**3.1. Analysis of single-population finite-size networks.** We start by investigating a single-population case. In the mean-field limit, we have shown that the infinite size system essentially exhibits the same behaviors as the WC model in terms of fixed points and limit cycles. But is this still the case where the number of neurons is finite?

At the bifurcations of the WC system, singular phenomena can occur. Consider for instance a saddle-node bifurcation point of WC system. At this point, the infinite size system will present a double zero eigenvalue, and the unfolding of this bifurcation can lead to different cases. As we show in this section, it can either unfold into a generic saddle-node bifurcation as we show in the first section, or it can generate an oscillatory behavior through a limit cycle, creating in the finite-size oscillations which do not exist in the WC or in the infinite size one population equations.

**3.1.1. Regular unfolding of the infinite-size system.** We start by considering BCC model with a strictly positive voltage to rate function  $f$ , and focus on acceptable solution that have positive firing rates and correlations. In that case, we numerically show that there is no qualitative difference between the stable solutions of the finite-size BCC network on one hand, and the infinite size system and WC system on the other hand (we showed that both models present the same qualitative behaviors in the one population case). We address this problem numerically, with an inactivation constant  $\alpha = 1$  (without loss of generality, since modifying this value only amounts rescaling time),  $w = 10$ , and letting both the size of the network  $n$  and the input parameter  $I$  free. The activity to rate function is chosen to be  $f(x) = 1/(1 + \exp(-x))$ .

With these parameters, WC system presents two saddle-node bifurcations when the input parameter  $I$  varies, as shown in Figure 3.1(a). The system therefore presents an interval of values of the parameter  $I$  where the system presents two stable fixed points and an unstable fixed point, and outside this interval, the system has a unique fixed point which is stable. Similarly to what we showed in the previous section, the infinite-size network presents exactly the same features, and no cycle.

We now study BCC finite-size equations. We set the size of the network to be  $N = 50$ . BCC finite size equations present the same qualitative behaviors, and the same type of bifurcations: the system undergoes two saddle-node bifurcations as the input parameter value  $I$  varies, and a bounded interval of input values  $I$  where the system presents a bistable behavior. The only qualitative distinction between finite-size networks and infinite size networks is the existence of a two unstable fixed points in the bistable zone and the fact that the system presents two distinct branches of fixed points, but these differences only affect unstable fixed points and do not produce generic qualitative differences in the behaviors.

The way this bifurcation diagram is transformed into the bifurcation diagram of the infinite system is very simple. The two distinct branches of fixed point get increasingly close, and in the limit  $n = 0$ , the two branches are superimposed. For finite-size networks, we observe that the value of the correlations of the stable fixed points was non-zero (see Fig. 3.1). These values were nevertheless quite small, and decrease towards zero as the size of the network as the number of neurons increases. When continuing the two identified saddle-node bifurcations as the network size increases, we observe that the bifurcation curve persists until the limit  $n = 0$  with no singularity. At the limit however, the non-zero eigenvalue of the Jacobian matrix at the saddle-node bifurcation point tangentially reaches the value 0 yielding the singularity predicted in proposition 2.2.

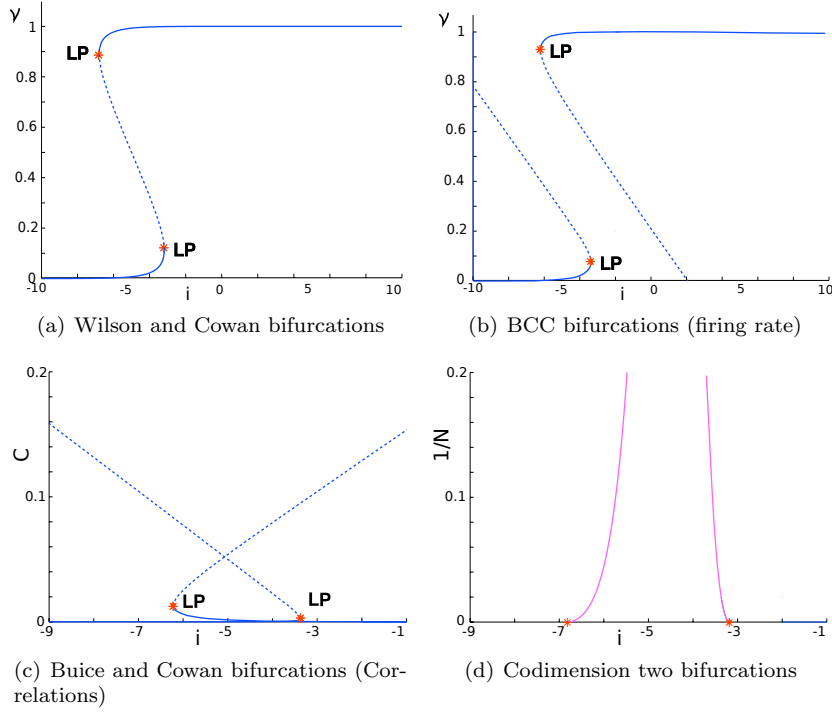


FIG. 3.1. *BCC model and the infinite-size system (a) Bifurcation diagram of WC system with respect to the input  $I$ . Plain curve: stable fixed point, dotted curve: unstable fixed points, LP stands for limit point (or saddle-node bifurcations) (b) and (c) Bifurcation diagram of BCC model with respect to  $I$ , for  $N = 50$  neurons. (b) Firing rates, (c) Correlations. (d) Codimension two bifurcation diagram with respect to  $I$  and the network size  $n = 1/N$ . Pink line: Saddle-node bifurcations (Limit Points). The star at  $n = 0$  denote double zero eigenvalue in the Jacobian matrix singular point. The values correspond to the values of WC saddle-node bifurcations.*

In this case, we therefore illustrated the fact that Buice and Cowan system can smoothly unfold the WC system by introducing correlations. These correlations vanish as the size of the population increases, yielding a purely Poisson firing with firing rates given by the solution of WC equations. For the same parameters and functions, it is easy to show, following the same steps, that Bressloff rescaled model also smoothly unfolds the WC system and that the finite-size system presents exactly the same type of bifurcations with two separated branches of fixed points each of which collapse in the limit where the number of neurons is infinite (not shown), and the value of the correlations of the fixed points decreases towards zero when the number of neurons increases. However in this case, one has to bear on mind that the interpretation of the result slightly differs: the limit behavior is now seen as a purely asynchronous state where all the neurons of the population fire independently in the limit  $N \rightarrow \infty$ . These behaviors will closely match the Markovian model's behavior as shown in section 3.1.1. In these cases, WC system conveniently summarizes the behavior of large networks, and provides a simple model to study large networks. However, there exist models for which this conclusion does not hold, and where the infinite-size system's behavior unfolds into more complex behaviors.

**3.1.2. Singular unfolding of the infinite-size system.** We now turn to study the possible singular unfolding of the infinite size system in one population. To this purpose, we will be specifically interested in studying oscillatory behaviors in the finite-size systems that are not present in the limit where the number of neurons tends to infinity. We will call these qualitative distinctions between finite-size and infinite-size systems singular unfolding.

To this purpose, we choose a framework where fixed points are easily described, and along the fixed point search for sufficient conditions to get a supercritical Hopf bifurcation, yielding oscillatory behaviors in single population networks that are neither present in the infinite-size system nor in the WC system. To fix ideas, similarly to the previous case treated, we consider BCC one population model. We consider here a non-physiological cases by allowing the firing rate variable to be negative. We choose an activation function  $f$  such that  $f(I) = 0$  for some fixed  $I$ , which can always be done with an unspecified sigmoid  $\tilde{f}$  through the modification  $f(x) = \tilde{f}(x) - \tilde{f}(I)$ . This quite unrealistic case will allow studying the qualitative differences that can appear between the finite and infinite size systems. However, the fixed point 0 is quite particular, and we will see that this phenomenon is not generalized in a simple way when considering positive activation functions  $f$  and positive firing rates (the affine transform  $\tilde{f}(x) - \tilde{f}(I)$  does not have a trivial effect on the nonlinear system).

BCC single population model reads:

$$\begin{cases} \frac{d\nu}{dt} &= -\alpha\nu + f(w\nu + I) + \frac{1}{2}f''(w\nu + I)w^2C \\ \frac{dC}{dt} &= -2\alpha C + 2f'(w\nu + I)w(C + \frac{1}{N}\nu) \end{cases}$$

Therefore, under the assumptions made, it is easy to see that the null solution  $\nu = 0, C = 0$  is always solution of the system. The Jacobian matrix  $J$  at this point reads:

$$\begin{pmatrix} -\alpha + w f'(s) & \frac{1}{2}f''(s)w^2 \\ 2f'(s)\frac{w}{N} & 2(-\alpha + w f'(s)) \end{pmatrix},$$

where we denoted  $s = w\nu + I = I$  for  $\nu = 0$ . The trace of the Jacobian matrix at this point is equal to  $3(-\alpha + w f'(s))$  and the determinant is equal to  $2(-\alpha + w f'(s))^2 - f'(s)f''(s)w^3/N$ . The trace vanishes at the null fixed point for  $(\alpha, w)$  such that

$$\alpha = w f'(I),$$

and therefore there exist a set of parameters for which the trace vanishes. In order to ensure that this null trace corresponds to the presence of a pair of purely imaginary eigenvalues, we further need to ensure that the determinant is strictly positive. When the trace vanishes, the determinant simply reads  $-f'(s)f''(s)w^3/N$ . Since  $f$  is a sigmoidal function,  $f'$  is always positive, and therefore the determinant is positive as soon as  $f''(s) < 0$ , which can be ensured for some specific firing rate functions. In that case, we will denote  $\omega_0 = \sqrt{-f'(s)f''(s)w^3/N}$ .

Therefore, under the assumptions that there exists  $I$  such that  $f(I) = 0$  and  $f''(I) < 0$ , there exist parameters  $\alpha$  and  $w$  such that the Jacobian matrix of the system at the null solution has a pair of purely imaginary eigenvalue. Let us now check that this point corresponds to a Hopf bifurcation when varying the parameter  $\alpha$ . To this purpose, we check transversality and genericity conditions of the Hopf bifurcation at this point, as given for instance in [24]. These calculations are provided in appendix C The transversality condition is easily checked. It consists in showing that the differential real part of the eigenvalues of the Jacobian matrix at this point,

with respect to the parameter  $\alpha$ , does not vanishes. Let us denote by  $\mu(\alpha)$  the real part of the eigenvalues. Since we are in a planar system, we have:

$$\begin{aligned}\mu(\alpha) &= \frac{1}{2}Tr(J) \\ &= \frac{3}{2}(-\alpha + w f'(s)) \\ \frac{d\mu(\alpha)}{d\alpha} &= -\frac{3}{2} < 0\end{aligned}$$

Therefore the transversality condition of the Hopf bifurcation is satisfied at this point. In order to fully state that the system undergoes a Hopf bifurcation, we need to show that the first Lyapunov exponent of the system at this point does not vanish. This Lyapunov exponent, after some tedious calculations using the formula given in [24] (see appendix C), is shown to be of the same sign as:

$$\frac{w^2 N}{f'(I)^2} \left[ f^{(3)}(I)f'(I) \left( 1 + \frac{1}{\omega_0} \right) + f''(I)^2 \left( \frac{2}{\omega_0} - \frac{14}{3} \right) \right].$$

The sign of this expression is governed by the values of the differentials of  $f$  at the point  $I$ . If the expression in the bracket is negative, then the Hopf bifurcation is supercritical and the system has stable oscillations. Let us now investigate the dependence of this cycle on the network size. We have shown that  $\omega_0 = \sqrt{-f'(s)f''(s)w^3/N}$ . Therefore, if this cycle appears for some finite network, it will lose stability as the size of the population increases. The period of the generated cycle is proportional to the inverse of the square root of  $N$ , and therefore slowly tends to zero as the network size increases (note that the cycle will lose stability as the network size increase, since for sufficiently large populations, the Hopf bifurcation will be subcritical).

Now that we identified simple conditions for the Hopf bifurcation to take place, we exhibit a network that indeed has this bifurcation. We choose for instance as activation function an hyperbolic tangent function

$$f(x) = \tanh(x) - \tanh(I)$$

with  $I = 0.5$ . In that case, we have:

$$\begin{cases} f(I) &= 0 \\ f'(I) &\approx 0.786 \\ f''(I) &\approx -0.727 < 0 \\ f'''(I) &\approx -0.56 \end{cases}$$

Therefore this function satisfies the assumptions done in the previous paragraph. Moreover, since  $f'''(I) < 0$  and  $(2/\omega_0 - \frac{14}{3}) < 0$  ( for  $N$  small enough), the first Lyapunov coefficient is negative, and therefore the system undergoes a supercritical Hopf bifurcation and presents oscillations, as illustrated in Figure 3.2.

Therefore, we exhibited a case where the finite-size equations have important qualitative differences from the infinite-size equations, and therefore where the mean-field limit does not efficiently summarizes the behavior of large columns. However this system involved non-physiological values of the parameters, and in particular involved a non-positive activation function  $f$ . Therefore, this behavior will never appear in the Markov process that yielded BCC equations. In order to exhibit a system with positive sigmoidal functions that indeed present oscillations in one-population networks,

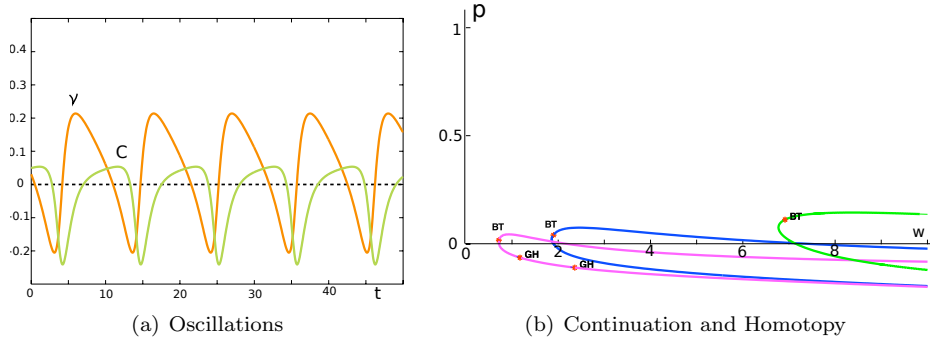


FIG. 3.2. *Oscillations in a single population network with finite size. (a) is a cycle observe for  $f_0$  ( $p=0$ ), (b) is the codimension two continuation with respect to  $w$  and  $p$  of the Hopf bifurcation for different values of  $\alpha$ : pink for  $\alpha = .3$ , blue:  $\alpha = .8$  and green:  $\alpha = 3$ .*

we aim at continuing the Hopf bifurcation and transforming continuously the sigmoidal transform into a positive function. For instance, we consider  $f$  a non-positive sigmoidal function for which the Hopf bifurcation exhibited here appears, and define  $f_p = f - p \min(f)$  a transformation of  $f$  such that  $f_0 = f$  and  $f_1$  is a positive sigmoid. This homotopic transform smoothly maps the vector field presenting an attractive cycle onto a vector field with a positive activation function. Since we have proved the genericity and transversality conditions on the Hopf bifurcation identified, we are in position to continue it as the parameter  $p$  varies together with  $\alpha$  in a codimension two bifurcation diagram (by application of the inverse function theorem). We observe in that case that the Hopf bifurcation cannot be continued when varying the homotopy parameter until reaching a positive sigmoid (see Figure 3.2(b) for the example provided above). We have tried numerous other sets of parameters and have never been able to continue periodic orbits to a regime where there is a non-negative activation function.

Therefore, though the one-population Buice and Cowan equations can display oscillations for non biologically relevant parameters, we conjecture that there is no acceptable oscillatory solution for positive activation functions.

**3.2. A two-populations finite-size network.** We have seen in the previous section that the one-population finite-size BCC model was accurately approximated by the infinite-size system (and therefore the WC system from the result of a previous section) for biologically realistic parameter, though oscillatory phenomena may occur for non-biologically relevant parameters that allow both the firing-rate and the correlations to be negative. The picture will be quite different in multi-population networks. Indeed, in higher dimensions, the WC system can have Hopf bifurcations that create very degenerate bifurcation points in the infinite-size system, which may non-trivially unfold in the finite-size systems. In this section, we consider the two population networks with excitatory self-interaction and negative feedback loop, called Model I, introduced in section 2.2.2 and address first the case of Bressloff model, before showing that BCC model presents the same features in appendix D.

With the parameters given in section 2.2.2, the two-population rescaled Bressloff

equations read, when denoting  $c = C$ :

$$\begin{cases} \nu'_1 &= -\alpha_1 \nu_1 + f(s_1) + \frac{1}{2} f''(s_1) (w_{11}^2 c_{11} + w_{12}^2 c_{22} + 2 w_{12} w_{11} c_{12}) \\ \nu'_2 &= -\alpha_2 \nu_2 + f(s_2) + \frac{1}{2} f''(s_2) (w_{22}^2 c_{22} + w_{21}^2 c_{11} + 2 w_{22} w_{21} c_{12}) \\ c'_{11} &= \frac{1}{N_1} [\alpha_1 \nu_1 + f(s_1)] - 2\alpha_1 c_{11} + 2 f'(s_1) (w_{11} c_{11} + w_{12} c_{12}) \\ c'_{22} &= \frac{1}{N_2} [\alpha_2 \nu_2 + f(s_2)] - 2\alpha_2 c_{22} + 2 f'(s_2) (w_{21} c_{12} + w_{22} c_{22}) \\ c'_{12} &= -(\alpha_1 + \alpha_2) c_{12} + f'(s_1) (w_{11} c_{12} + w_{12} c_{22}) \\ &\quad + f'(s_2) (w_{21} c_{11} + w_{22} c_{12}) \end{cases}$$

where we denoted:

$$\begin{cases} s_1 &= w_{11} \nu_1 + w_{12} \nu_2 + i_1 \\ s_2 &= w_{21} \nu_2 + w_{22} \nu_2 + i_2 \end{cases}$$

For the set of parameters studied in this section and a number of neurons  $N = 50$ , Bressloff finite-size system undergoes four Hopf bifurcations labelled H1 through H4 and six saddle node bifurcations LP1 through LP6. It features two distinct families of limit cycles, one that undergoes two folds of limit cycles LPC1 and LPC2, and one that undergoes a Neimark-Sacker (Torus) bifurcation, as displayed in Figure 3.3(b), and are compared with the standard WC system that displays one Hopf bifurcation point H and two saddle node bifurcations LPa and LPb.

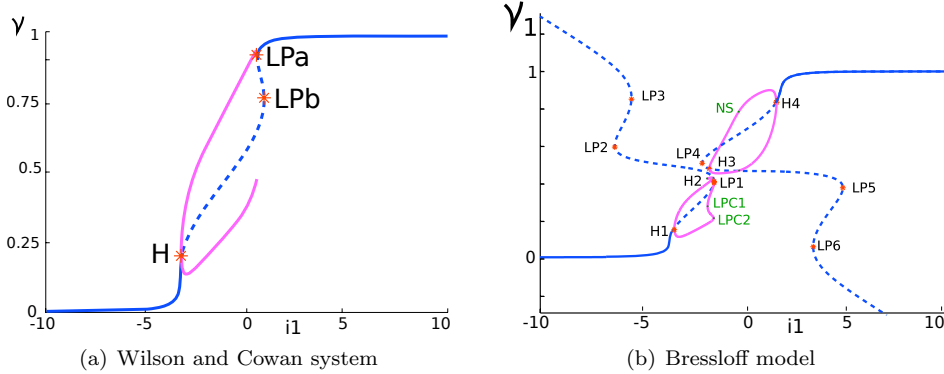


FIG. 3.3. *Bifurcation diagram of Model I: (a) Wilson and Cowan system and (b) Bressloff system. Blue: equilibria, pink: cycles. Bifurcations of equilibria are denoted with a red star, LP represents a saddle-node bifurcation (Limit Point), H a Hopf bifurcation. The four Hopf bifurcations share two families of limit cycles. One of these undergoes two fold of limit cycles LPC, and the other branch of limit cycle a Neimark Sacker (Torus) bifurcation.*

The analysis of this bifurcation illustrates the fact that the small finite-size system studied have clear qualitative differences with the WC system. However, because of the properties of the vector field, and in particular its smooth dependency with respect to the size of the network  $N$ , the bifurcation diagram of Fig. 3.3 smoothly connects to the degenerate bifurcation diagram of the infinite-size system presented in section 2.2.2.

Let us now investigate how the bifurcation diagram of the infinite system unfolds to the bifurcation diagram of the finite-size system. To this end, we continue of the bifurcation diagram of figure 3.3(b) as the number of neurons increases, as shown

in the codimension two bifurcation diagram of Figure 3.4. It appears that the form of the bifurcation diagram remains similar to the one presented in Fig.3.3 for any network smaller than 232 neurons ( $n_2 = 0.0867$ ), and features the same number and type of fixed points, cycles and bifurcations. At this size of the network, the system undergoes a cusp bifurcation, generating two saddle-node bifurcations denoted LP7 and LP8 on the right branch of fixed point. The value of the correlation variables of these points progressively converge to zero as the network size increases. These two saddle-node bifurcations correspond in the infinite-size limit to the two saddle nodes of WC system LPa and LPb, and are not present in the finite-size model for a small number of neurons. All other bifurcations observed in the diagram of Fig. 3.3 are continued for any network size, and the correlations do not vanish. However, these bifurcations arise on unstable fixed points and do not present any stable behaviors. The branch of fixed points corresponding to smaller values of the input parameter  $I_1$  connects to the second branch of fixed points corresponding to larger values of  $I_1$  in the mean-field limit and collapsing on the zero correlation space. The set of bifurcations arising on unstable branches of fixed points only correspond to unstable solutions and are not plotted. The continuation the Hopf bifurcation labelled H1 in

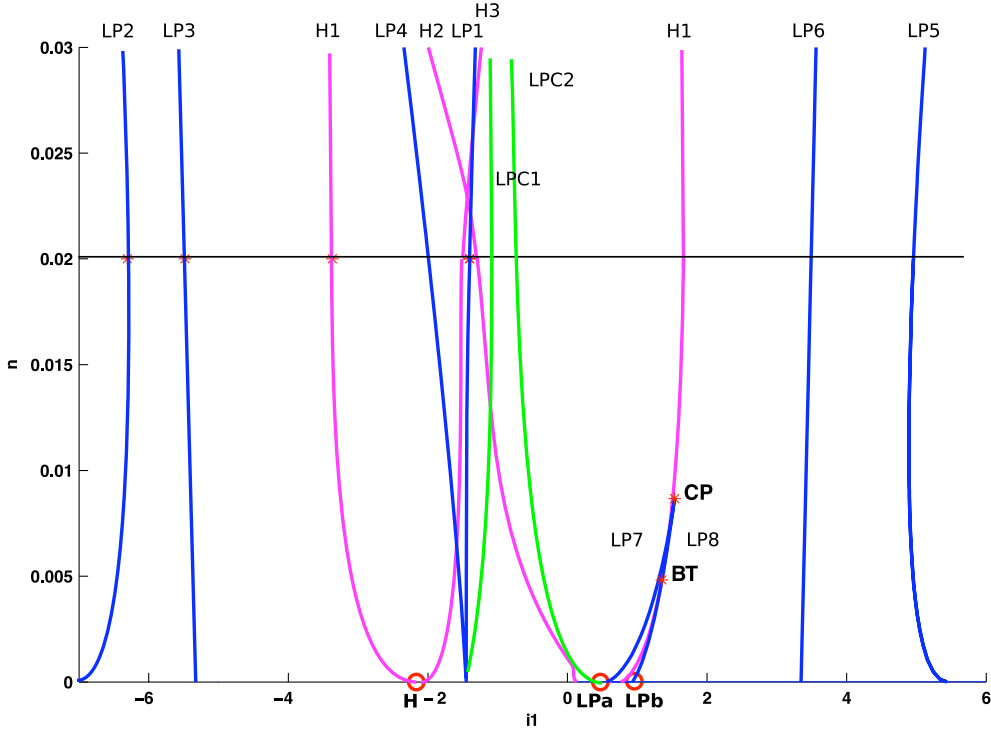


FIG. 3.4. Codimension two bifurcations with respect to the input to population 1 and the population size in Bressloff's model. Pink: Hopf bifurcations, blue: saddle node bifurcations, green: folds of limit cycles. Hopf bifurcations, when continued, merge pairwise in the infinite-size system. We observe that the fold of limit cycles merge with other bifurcations in the limit of infinitely many neurons (see text). In the limit  $N \rightarrow \infty$  (corresponding to  $n = 0$ ) we labelled the points H, LPa and LPb arising in WC system. Points with zero correlations are circled in red, all other points have non-zero correlations.

diagram of Fig. 3.3(b) is continued as the network size increases and collapses in the limit  $N \rightarrow \infty$  with the continuation of the Hopf bifurcation H3 of the second branch

of fixed point. Their collapse corresponds to the degenerate Hopf bifurcation point of the infinite model, denoted H in Fig. 3.3(a). The cycle originating from H1 and the cycle originating from H3 will therefore emerge from this fixed point. This is why from the degenerate Hopf bifurcation point of the infinite system, two cycles emerge, as observed in the study of the infinite-size system in Fig. 2.1. This structure accounts for the fact that exactly two distinct cycles appear at the point H in the infinite-size system. The cycle originating from H3 undergoes a Neimark-Sacker bifurcation that can be continued in the mean-field limit, and corresponds to the loss of stability of this cycle. This cycle undergoes an additional period-doubling bifurcation when the size of the network increases, as observed in the bifurcation diagram of the infinite-size system, and as shown in figure 3.5. In that figure, we continued these cycles for one fixed value of the parameter  $I_1 = -0.5$ , as the number of neuron increases. The family of limit cycles continued is stable in a bounded interval of values for the parameter  $N$ . For a number of neurons close to  $N = 142$  (precisely  $n_2 = 0.01418$ ), the branch of limit cycles undergoes a fold of limit cycle, and therefore the branch of limit cycles does not exist for smaller networks. For networks larger than  $N = 142$  neurons, the system presents a branch of stable and a branch of unstable limit cycles. Stable cycles persist up to networks as large as  $N = 1700$  neurons (precisely  $n_2 = 0.001174$ ). At this size, where the branch stable limit cycles changes stability through a subcritical Neimark Saker (Torus) bifurcation with no strong resonance. When increasing further the size of the network, the system has chaotic behavior which is clearly non-existent in the two-dimensional WC system, yielding an important qualitative distinction between large scale networks and the relative mean-field limit (see 3.5). This chaotic behavior exists until the infinite-size is reached. The branch of limit cycles arising from H3

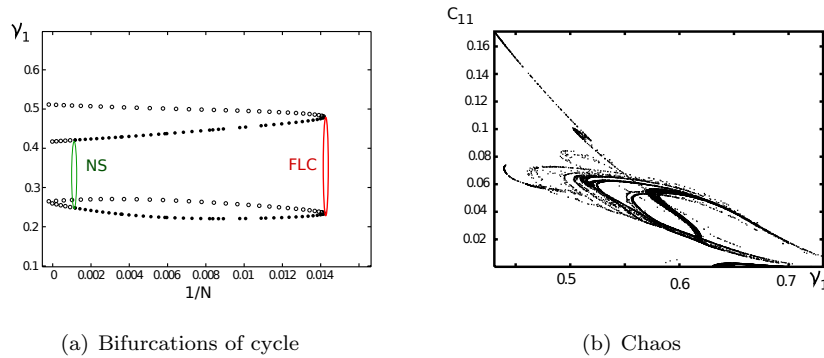


FIG. 3.5. Chaotic behavior for large networks: (a) bifurcation diagram as a function of the network size. NS: Neimark-Sacker (Torus) bifurcation and FLC: fold of limit cycle. (b) Poincaré maps representing  $a_1$  and  $c_{11}$  with Poincaré section  $a_2 = 0.7$ .

disappears in the diagram of Fig. 3.3 on the Hopf bifurcation point labelled H4. When continuing H4, we observe that the Hopf bifurcation is maintained whatever the network size, and in the mean-field limit collapses with the continuation of the Hopf bifurcation H2. Therefore, there exists in the infinite-size system an additional degenerate Hopf bifurcation that generates cycles with non-zero correlations. This Hopf bifurcation takes place on a unstable fixed point manifold and does not appear as stable solutions of the system, and accounts for the vanishing point of the additional cycle observed in the bifurcation diagram of the infinite-size system. Note that this

point where H4 and H2 merge has a non-zero correlation.

Let us now consider the continuation of the saddle-node bifurcations. The bifurcation diagram of WC presents two saddle-node bifurcations LPa and LPb that correspond to the two saddle-node arising from the cusp bifurcation CP of Fig.3.3 that are labelled LP7 and LP8. In the mean-field limit, the saddle-node bifurcations corresponding to the continuation of LP1 and LP4 merge in a cusp bifurcation and disappear. At this same point, the fold of limit cycles LPC1 collapses and disappears in a saddle-node homoclinic bifurcation. The saddle-node bifurcations LP2 and LP6 disappear in the mean-field limit by being continued tangentially to the line  $n = 0$ . The continuations of the saddle-node bifurcations LP3 and LP6 crosses the line  $n = 0$  with no singularity and therefore exists in the infinite size system, corresponding to a non-zero correlation saddle-node bifurcation that arise on an unstable fixed points manifold. Eventually, the saddle-node bifurcation LP7 connects with the fold of limit cycle, generating the saddle-node homoclinic bifurcation of the infinite-size system.

We therefore observe that the bifurcation diagram of the finite-size Bressloff model non-trivially unfolds the infinite-size system, and that at any finite scale the bifurcation diagram and the solutions it present differ significantly from the infinite-size system and from WC system. In particular, it shows additional cycles, as observed in the infinite-size system previously, and a chaotic effect that is not present in the two-dimensional WC system. This analysis also illustrates a mesoscopic-scale phenomenon in the presence of a periodic orbit that is stable only when the size of the network is comprised roughly between one hundred and one thousand neurons, a typical size of a cortical columns often modelled by Wilson and Cowan system. These results remain valid for BCC model, as shown in appendix D. The question that now arises is whether these behaviors indeed reflect behaviors of the Markovian model.

**3.3. Finite-size Markovian model.** In the previous section, we investigated the distinctions between the solutions of the finite-size Bressloff model and compared these with those of the infinite-size and of WC systems. We now return back to the original Markovian system that allowed derivation of Bressloff and BCC equations, and compare simulations of this network with the finite-size Bressloff model, composed of two differential equations arising from the moment truncation of this random variable. We will perform this analysis in the two models with two populations investigated in the paper, Model I and Model II.

In order to simulate the Markov chain, we make use of Doob-Gillespie's algorithm [15, 21, 22]. From the master equation (A.1), we derive the transition rates of the state variable  $n$ . We use these rates to simulate sample paths of the state variable  $n$  and rescale these to compare to the solutions obtained for BCC or Bressloff models and the infinite-size models. Given the configuration  $n(t)$  of the network at time  $t$ , we have:

- The probabilistic intensity for the transition  $n_i(t+1) = n_i(t) - 1$  is equal to  $q_i = \alpha_i n_i$ ,
- The probabilistic intensity for the transition  $n_i(t+1) = n_i(t) + 1$  is equal to  $f_i = f(\sum_{j=1}^M w_{ij} n_j + I_i)$ .

Given an initial condition  $n(0)$ , a simulation consists of computing all possible transitions probabilities  $q_i$  and  $f_i$ . We then draw the time for the next transition as an exponential random variable with intensity  $Q = \sum_i (q_i + f_i)$ . This time provides the next event occurring in the chain. By the properties of exponential laws, the transition is  $n_i(t+1) = n_i(t) - 1$  (resp.  $n_i(t+1) = n_i(t) + 1$ ) for some  $i \in \{1, \dots, M\}$  with probability  $q_i/Q$  (resp.  $f_i/Q$ ). This simulation algorithm for the Markov process  $n(t)$

is exact in law, and does not involve any approximation such as time-discretization, and therefore allows efficient simulation of the sample path and of its statistics. These statistics are computed using a Monte-Carlo algorithm consisting of simulating many independent sample paths of the process and deriving from these the trajectory of the mean firing rate  $\nu_i(t)$  and the correlation in the firing activity  $C_{i,j}(t)$  through the empirical mean and correlations obtained.

**3.3.1. One-Population Model.** We start by considering the one-population model studied in section 3.1.1. In that case we have shown that both Wilson and Cowan and the infinite-size systems had the same behavior, and that this behavior was regularly unfolded in the finite-size systems. In these cases, two saddle-node bifurcations defined a zone of bistability that depended on the size of the network as shown in Figure 3.1(d). We simulate the network using Doob-Gillespie algorithm and identify the boundaries of the zones where bistability occurs by continuation of the fixed points obtained as the parameters increase or decrease. The continuation is initialized by running the algorithm with parameters associated to a single attractive fixed point of WC system. Then the parameter  $I$  is slowly varied and simulations are run with initial condition being the last values of the network state of the previous simulation. We observe the hysteresis phenomenon and bistability, and the bistability zones closely matches WC system, as shown in Figure 3.6. Note that we numerically observe that the Markov chain converges towards an asynchronous state as illustrated by the value of the correlations being close to zero, and therefore compare the results of the Markov simulations with boundaries obtained in the bifurcation diagram of Bressloff's system for consistency. We simulate the network for increasingly large

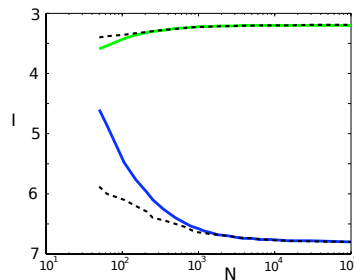


FIG. 3.6. *Bistability zones in Bressloff finite-size model (black dashed curve) and computed from the Markovian model (colored plain curve).*

networks ranging from  $N = 50$  neurons to  $N = 100\,000$  neurons with 10 000 simulated sample path from which we extract the empirical mean and standard deviations. From the curves obtained in that fashion, we automatically identify zones where there is bistability. These boundaries are plotted together with the values of the saddle-node bifurcation at these points arising from the codimension 2 bifurcation diagram of BCC model, and we observe that the curves closely match as soon as the network is larger than 1 000 neurons. Therefore in this model, Bressloff system closely reproduces the behavior of the finite-size Markov model for sufficiently large networks.

**3.3.2. Markovian Model I.** We now turn to study the two-dimensional network Model I. In that case we showed that depending on the input parameter  $I_1$ , Wilson and Cowan system can either present a stable cycle or a stable fixed point. We first chose a case where WC system converges towards a fixed point, and to this

end will study the system for  $I_1 = -5$ . In that case, both WC system, the infinite-size system and BCC (or Bressloff) system converge towards a fixed point. We will then address the case of periodic orbits in the Markovian system, and study Model I with  $I_1 = -2$ . In that case, we observed that WC system presented a cycle which lost stability in the infinite-size system in favor of an additional cycle featuring non-zero correlations. This cycle has a counterpart in the finite-size system, which allows identifying parameters and initial conditions<sup>2</sup> related to it. Simulations of the network will therefore allow discriminating which model best summarizes the activity of the population, and if the truncation hierarchy up to the second order indeed provides a good model of the network.

*Fixed points.* We first investigate the case where WC system presents a unique hyperbolic attractive fixed point. We showed that in this case, the infinite-size presents an exponentially stable fixed point with the same values of mean firing rate and null correlations, which has a counterpart in the unfolding of BCC and Bressloff model. Simulations of the Markovian model shows that all sample path of the process converges quite fast towards this fixed point with null correlations displaying stochastic variations, and each sample path presents a precise match with the solution of WC solution at this point. All stochastic variations around Wilson and Cowan trajectory are averaged and produce a fixed firing rate corresponding to the fixed point of the infinite-size system, i.e. having null correlations and the same value of mean firing rates. In that case, it appears that WC system provides a good model for the solutions of the Markovian model. Besides, we observe that the correlations vanish, which implies that the state obtained is an asynchronous state. Figure 3.7 represents simulations of Model I with  $I_1 = -5$ . In panels (a) and (b) are plotted four sample paths of the process for 10 000 neurons simulated over on a time interval equal to 100, and panels (c) and (d) the mean-firing rates averaged over 5 000 realization of the process, and that shows a very close agreement with the solution of WC system. The maximal absolute value of the correlations (not plotted) are of the order of  $10^{-5}$  and are neglected as an effect of the finiteness of the sample path simulated for computing the mean and covariance. The same observations hold for all the simulations performed for parameters corresponding to an hyperbolic fixed point of the infinite system. Note that the difference between mean-firing rates of the solution of WC system on one hand and of Bressloff system on the other hand is of the order of  $10^{-5}$  at this network scale, and therefore both models fairly approximate the stochastic Markovian model.

*Cycles.* We now turn to study periodic orbits in the Markovian system and compare it with the differential equations that approximate these. We perform simulations of 1000 sample paths of the Markovian network associated with Model I with  $I_1 = -2$  featuring 100 000 neurons. For these parameters, as already stated, we observed that Bressloff's and BCC models differ from a pure WC system, and yield a different stable oscillatory behavior with non-zero correlations. We compare the solutions of the simulated Markov chain in order to discuss which model better matches the behavior of the stochastic process of spikes.

We start by considering individual trajectories of the Markov chain. We observe that each of these sample paths closely coincide with the solution of WC systems, as displayed in Figure 3.8. However, as a time goes by, the stochastic nature of the

---

<sup>2</sup>Note that the finite- and infinite-size systems have five initial conditions: the initial firing rates and correlations, but the Markov chain is initialized by defining the number of active neurons in each populations, and the correlations cannot be initialized.

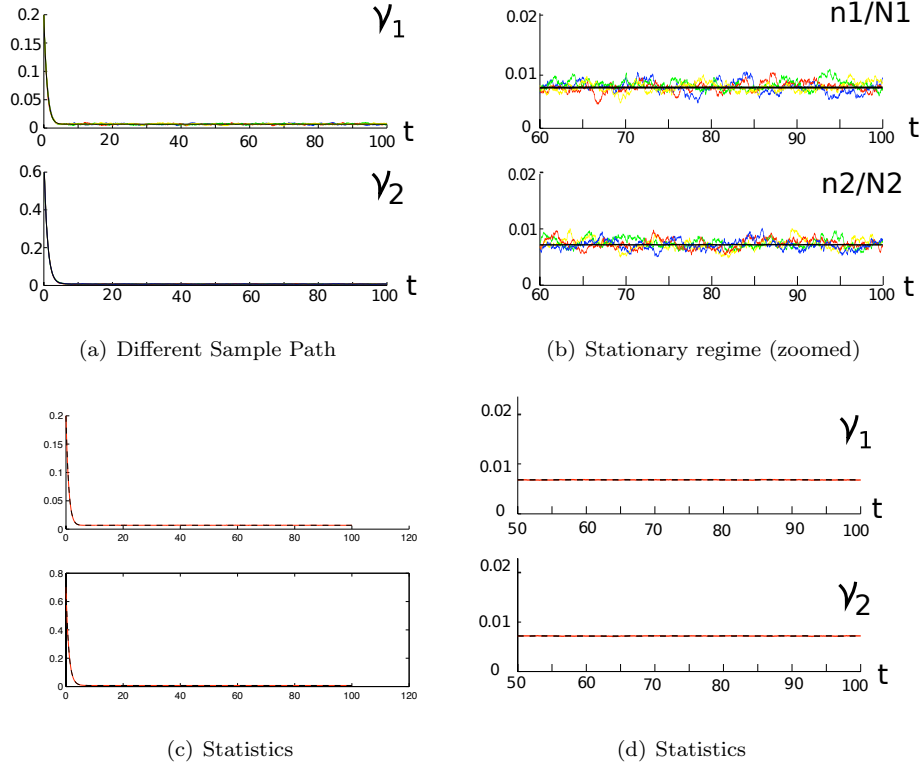


FIG. 3.7. *Network Model I*, for parameters associated with a stable fixed point ( $I_1 = -5$ ) closely matches WC trajectory with random variations around the fixed point that average at the value of the fixed point, and correlations vanish (asynchronous state). (a),(b): The different colors correspond to different sample paths.

process produces stochastic phase differences in the oscillations, and each sample path slowly deviates from the solution of WC system, while the trajectory of the sample path in the phase plane ( $\nu_1, \nu_2$ ) conserves a good match with Wilson and Cowan cycle. We conclude that each neuronal population evolves closely to WC cycle (oscillating with the same frequency), and coincides with it very closely at small time scales (up to 30 periods of WC cycle). Therefore, we can see that Wilson and Cowan appears as a good deterministic model of the stochastic activity of the population itself, even after very long times. WC system is therefore a simple model efficiently summarizing the behavior of the random variable  $n(t)$  (see Figure 3.8). Let us now consider the statistics of the random state variable  $n$ . We observed in Figure 3.8 that the different samples of the activity variable are transiently synchronized through different realizations of the Markov chain. This transient synchronized phase is increasingly long as the size of the network increases, and has a very good match with the solution of WC equation starting at the same initial condition. Therefore, the mean firing rate during this period will keep close to the solution of WC system. However, though oscillating around the same cycle during all the evolution of the process, we noted that the time evolution of each sample path deviated from a pure solution of WC system because of the stochasticity of the system, and a stochastic phase difference appeared between different sample paths. The presence of this stochastic phase difference will

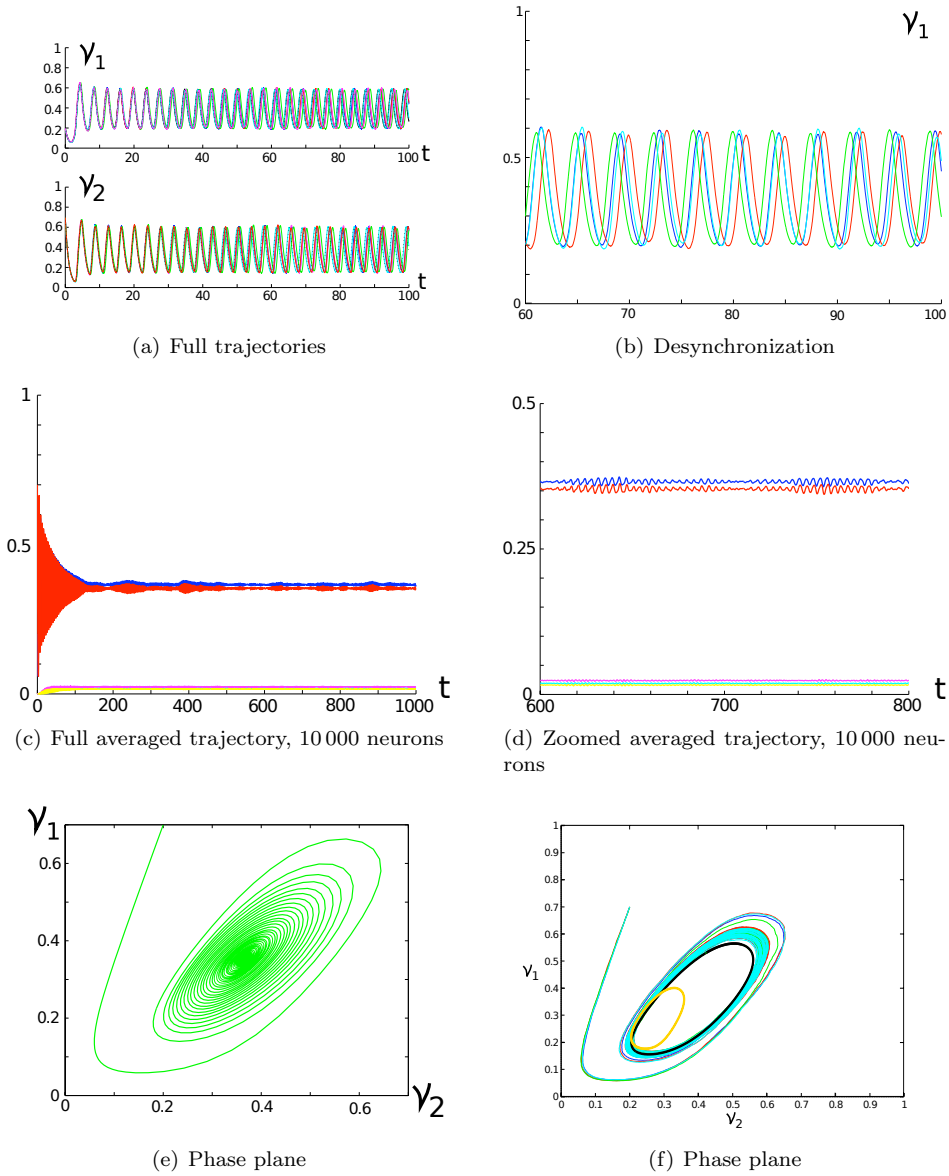


FIG. 3.8. Simulation of four sample paths of the Markovian model in the case of Model I with  $I_1 = -2$  and the same initial condition (a),(b),(e) and averaged trajectories (c,d,f). We observe that all trajectories (solid colored curves) show oscillations corresponding to WC cycle (black dotted curve in (a)), that slowly shows a stochastic desynchronization (b), but always keep oscillating close to WC system (c). The different colors correspond to four different sample paths. Time of the simulation: 100, Number of neurons: 100 000. The averaged activity is computed over 1000 realizations of the process for 10 000 neurons, initially matches WC cycle and keeps oscillating with a decreasing amplitude as time goes by to reach a fixed point with non zero correlations

therefore produce differences between the behavior of a given sample path and the mean activity averaged over many realizations. When computing the averaged value of the state variable and of the correlations over 5000 simulated sample paths of the

Markov chain with 100 000 neurons starting at the same initial condition, we observe indeed that if the averaged activity is initially well approximated by the solution of Wilson and Cowan system, it slowly deviates from it, by keeping oscillating at the same frequency but with increasingly small amplitude. And instead of obtaining after the transient phase the cycle expected from the analysis of the finite-size BCC and Bressloff models, we record that the asymptotic behavior of the system, after a long transient time, corresponds to a fixed point with constant firing rates corresponding to the mean values of WC cycle, and constant non-zero correlations (see Figure 3.8). We conclude from this numerical analysis that the truncation hierarchy up the second moment does not fully capture the behavior of the Markov chain, and one has to choose another method to approximate the behavior of the chain. This fact will be further analyzed in the discussion. We eventually note that in the case studied here, the limit behavior appears to be a stochastic random variable, that neither corresponds to an asynchronous state (since correlations do not vanish) nor a Poisson firing state. We also observe in this case that the two first moments or the two first ordered cumulants (as well as any same-time moment of the chain) are not enough to describe the law of the firing activity in the stochastic process. Indeed, the law appears to be a stochastic perturbation of a cycle, and all the moments, because of the phase shifts in the oscillations of each sample path, will be constant. In order to better describe its behavior, it is essential to take into account the correlations between different times. For instance, we observe that the correlations

$$\tilde{C}_{ij}(t, s) = \left\langle \frac{n_i(t)}{N_i} \frac{n_j(s)}{N_j} \right\rangle - \nu_i(t) \nu_j(s).$$

After a long transient time, we consider the stationary state reached by the Markov chain. We compute the correlation functions in the case of our simulations, and plot  $C_{11}(t, s)$  as a function of  $t - s$ . We observe that this plot corresponds to a curve with a non-trivial quasi-periodic shape corresponding to the stationary state of the chain (see Figure 3.9).

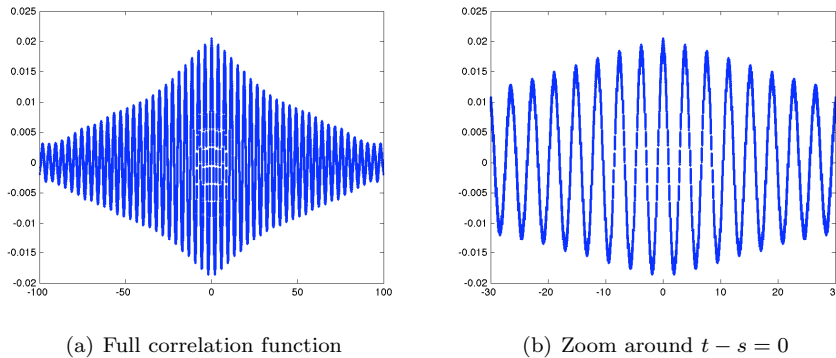


FIG. 3.9. Correlations  $\tilde{C}_{11}(t, s)$  as a function of  $t - s$  (each value  $\tilde{C}(t, s)$  for  $(t, s) \in [400, 500]^2$  provides a point of the graph with abscissa  $t - s$ ). For each value of  $t - s$ , multiple points are plotted. These appear to be superimposed (there are multiple points for a given value of  $t - s$ ). The obtained function is an oscillation whose amplitude decreases as  $|t - s|$  increases.

**3.3.3. Markovian Model II.** We perform the same analysis in the case of the network Model II studied in section 2.2.2 with symmetric connectivity with null diag-

onal and inhibitory interaction. In that case, we showed that WC system presented bistability, and the infinite-size system presented a more complex behavior with multistability and different limit cycles. In the simulations of the Markovian system, similarly to the case of Model I, we observe that when WC system presents a single hyperbolic fixed point, the Markovian closely matches with the solution of WC system during the transient phase, and the stationary state randomly varies around the fixed point of WC system. The mean of the firing rates over many realization of the process converges exactly towards the solution of WC system, and the correlations tend to zero, implying the system is in an asynchronous state and that its behavior is efficiently summarized by Wilson and Cowan system. We note that in that case, the infinite-size system and the finite size systems both presented additional fixed points with non-zero correlations, that do not actually exist as a regime of the Markov chain.

For parameters associated with bistability in WC, the situation is similar, and we observe in our simulations that the WC system captures precisely the behavior of the Markovian system and all additional solutions derived from the moment hierarchy truncation do not appear. Simulations of the Markovian system show that depending on the initial condition, the system will converge towards one or the other fixed point. Albeit the stochasticity of the Markov chain yielding the possibility to switch between the two fixed points, this phenomenon does not occurs often, and except for input parameters very close to the saddle-node bifurcations, no switching between fixed points is observed. In that case again, the additional fixed point with non-zero correlations and the additional cycles evidenced in the infinite-size system and that are present in the finite-size BCC and Bressloff equations do not appear in the Markov model. We present in Figure 3.10 the values of taken by the mean firing rate and correlations for 1000 realizations of the Markov chain over the 20 last units of time for a simulation of 20 000 neurons as a function of the input parameter  $I_1$ . We treat the cases  $I_2 = 0$  and  $I_2 = 5$ , the blue crosses are the continuation of the fixed points with  $I_1$  increasing (from  $-10$  to  $10$  for  $I_2 = 0$  and from  $-5$  to  $15$  for  $I_2 = 5$ ) and red circles for  $I_1$  decreasing. The continuation is initialized by running the algorithm with parameters associated to a single attractive fixed point of WC system. Then the parameter  $I_1$  is slowly varied and simulations are run with initial condition being the last values of the network state of the previous simulation. We observe the hysteresis phenomenon and bistability, and the bifurcation diagram obtained perfectly matches WC's, and no counterpart of any of the identified correlations effects are observed.

Therefore, we conclude in that case again that WC equations constitute a better model to describe the dynamics, since the correlation-induced and finite-size effects observed in BCC and Bressloff models do not appear in the simulations of the network. All these observations raise some new questions on the dynamics observed in the finite- and infinite-size equations derived from moment expansions of the Markov model we now turn to discuss.

**4. Discussion.** In this paper, we studied the different solutions of newly developed models for describing the mean-field limit of Markovian neural networks modeling large-scale cortical areas: BCC and Bressloff models[12, 7]. These equations are derived from a Markovian implementation of the firing of each neurons in the population, whose transition probability satisfied a differential equation, the master equation of the process[16]. Both models studied drew on this framework, and after truncation of the moment hierarchy yielded sets two coupled equations, one governing the mean firing activity and the other governing the same-time correlations of the firing activity in the network (or the ordered cumulant that can be deduced from the correlation

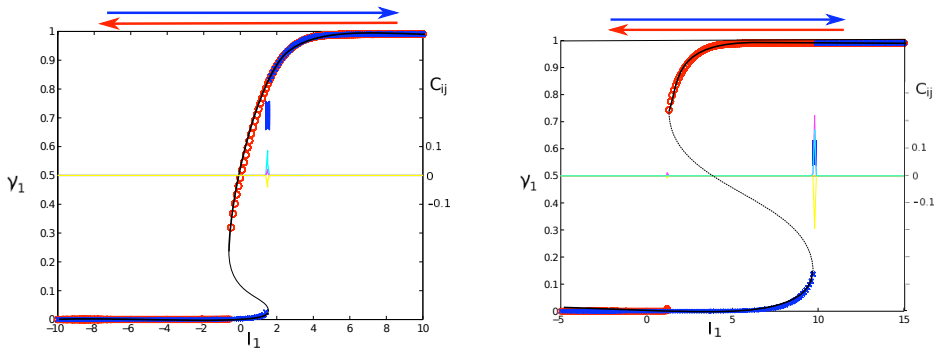


FIG. 3.10. Stationary values of the Markov chain in Model II with  $I_2 = 0$  as a function of  $I_1$  (see text). Continuation of equilibria by increasing  $I_1$  (blue crosses) and by decreasing  $I_1$  (red circles), superimposed with WC bifurcation diagram (black curve). Correlations are plotted with a different axis origin in cyan ( $C_{11}$ ), magenta ( $C_{22}$ ) and yellow ( $C_{12}$ ), keep very close to zero except at the precise value of the bifurcations, where the jump between the two fixed points produces a spurious standard deviation.

and the mean firing rate). The particular aim of both models was to recover, in the limit where the number of neurons is infinite, the standard WC equations.

We extended these models to study networks composed of different populations of neurons with different dynamics and composed of different number of neurons. Both models include finite-size corrections, and the size of the network appears simply in the equations as a parameter of the model. The limit when the number of neurons tend to infinity appears in that view as a regular perturbation of the finite-size system. We observed that both BCC and Bressloff models converged towards the same equations as the number of neurons tend to infinity, the infinite-size system.

We analyzed the solutions of the infinite-size system, and established the fact that all solutions of WC system were associated with solutions of the infinite-size system with null correlations. However, we showed that the stability of the solutions obtained in that fashion did not necessarily have the same stability properties as in WC system: fixed points of the Wilson and Cowan system correspond to fixed points of the infinite-size system with zero correlations having the same stability, but all the cycles of the WC system are either unstable or neutrally stable in the infinite-size system. This destabilization of cycles gives rise to new behaviors (fixed points or periodic orbits) with non-zero correlations, the correlation-induced behaviors.

When studying the finite-size equations and the way it relates to the properties of the infinite-size system, we presented evidence that the mean-field limit appears to be a singular limit, in the sense that for any finite-size of the network, the system presents behaviors the infinite-size system does not feature. Moreover, singular points appear in the limit of infinitely many neurons, and for infinitely many neurons, branches of bifurcations collapse and disappear. Besides these qualitative distinctions between finite and infinite-size systems, we numerically found mesoscopic-scale effects, namely behaviors that are only present at a certain population scale, and disappear for smaller or larger populations. The scale at which these behaviors took place coincided with the scale of typical cortical columns. Such behaviors are neither captured by the study of small-networks nor by the mean-field limit, stressing the importance of precise descriptions of these intermediate scales in tractable approaches.

Correlation-induced and finite-size behaviors were then compared to the initial

Markovian model. We observed that when WC system presented an attractive fixed-point behavior, each sample path of the Markov chain presented stochastic variations around these fixed points, the correlations tended towards zero and the mean coincided with WC fixed point. In that case, the network regime is therefore an asynchronous state, and is well approximated by Wilson and Cowan system. The infinite-size system also features the same fixed point, and therefore captures this behavior. Moreover, the dependency of the fixed point bifurcation on the size of the network was closely matched with the simulations of the Markovian system, hence Bressloff and BCC equations are good models of the Markovian network in fixed point regimes. It is important to note that both BCC and Bressloff models can present additional behaviors in these regimes that are not present in the simulations of the Markov chain. When considering periodic orbits of WC system, the conclusion substantially differs. We indeed observed that each sample path presented a good agreement with WC system with stochastic differences that averaged to a fixed point, which is neither present in WC system nor in BCC and Bressloff models. The behavior of the stochastic firing rate in each realization of the process is therefore well represented by solutions of Wilson and Cowan system, but the averaged firing rate converges towards a fixed point that is present in none of the presented models. In the case where the firing rate of the Markov chain appears as a stochastic phase shift in the oscillations of the WC system, the zero-time correlations  $C_{ij}(0)$  are not sufficient to describe the dynamics and more refined descriptions are needed.

We conclude from this study that the equations obtained by the moment hierarchy truncation efficiently summarizes the behavior of the Markov chain in fixed-points regimes, but fails in reproducing the behavior of the Markov chain in oscillatory regimes. This can be linked with the choice of variables used to describe the state of the system. We indeed noted in the introduction that the correlations taken into account in these models are only considered at for the firing occurring exactly at the same time ( $c_{ij}(t) = \langle n_i(t) n_j(t) \rangle$ ) in contrast to the full 2-variable correlation functions  $\tilde{C}_{i,j}(t, s) = \langle n_i(t) n_j(s) \rangle$ . This is quite a rough approximation for stochastic processes, since the presence of infinitely many neurons tends to increase the memory of the system and to produce long-term correlations. For instance, Faugeras, Touboul *et al* [20] showed that the mean-field limit arising from a network of stochastic Wilson and Cowan systems involves an infinite-time memory term corresponding to the limit of the interaction process between each populations, making the mean-field limit a non-Markovian system. Taking into account the full correlation function makes the system dramatically more complex, involving implicit integral equations on the correlations and whose solutions would probably diverge from the solutions obtained in BCC and Bressloff model.

A hypothesis we propose to account for the discrepancy between correlation-induced behaviors and actual behaviors of the Markov chain is linked with the moment truncation. Such methods indeed have been widely discussed, and sometimes their validity is not ensured. For instance, for other models, Ly and Tranchina [27] showed that the moment closure in a population density approach to derive mean-field limits was ill-posed. In the case of the models studied in the present paper, even though Bressloff showed that  $m$ th order moment contributed with a coefficient equal to  $1/N^{m/2}$ , there is at any scale an infinite number of moments, that can produce significant nonlinear contributions to the equations. Uncovering how these contributions evolves as  $N$  increases involves a double limit, one on the moments taken into account and one on the size of the network, that can be very complex. We believe

that finite-size and correlation-induced effects observed can be artifactual solutions arising from the approximations made in the moment truncation.

We recall that the choice of the activation and inactivation functions in the Markovian model was mainly driven by the aim to get WC equations in the mean-field limit. However, this choice was not exclusive, and involves an arbitrary definition. This point is interestingly stressed by Bressloff in [7]: there exists an infinite-dimensional degree of freedom in the derivation of the equations that do not affect the mean firing rate equations (therefore yielding WC equations in the mean-field limit) that strongly affects the equation on the correlations. This function is arbitrarily chosen to be zero in Bressloff model, as he explicitly mentions, and this choice was driven by the simplicity of the mean-field equations obtained. Solutions of the finite- and infinite-size systems can therefore differ from the one obtained in the choice  $\Gamma \equiv 0$  and maybe a suitable choice of this function can yield the observed behavior. We unfortunately lack interpretation for this function, and therefore it is very difficult to arbitrarily make a suitable choice, and more investigation is needed in this domain to understand the meaning and possible relevant forms of this function.

The precise study of all these points will further allow understanding the behavior of large scale systems, and will particularly be interesting in the study of rhythms in the brain, and possible synchronization or desynchronization as a function of the network size and of the connectivity. A particularly interesting point of the models studied in this paper is that it describes a stochastic process by a set of differential equations, where the size of the network appeared as a perturbation parameter of a set of ordinary differential equations. This approach can be promising in order to study bifurcations of a stochastic processes and qualitatively analyzing its behaviors and the dependency of its solutions as a function of the parameters. We also noted that the behavior of each sample path of the process was possibly very different from the behavior of its first moments, which raises the question of the best variable to describe such stochastic processes.

The mathematical method developed to study the stability of the correlation equations, involving Kronecker products and sum and the application of Floquet theory is of potential big importance in the study of networks with correlations, since the form of the correlation equation is quite standard in this kind of problems (see e.g. [31] in the case of small noise expansion). This approach can also be applied to the study of the stability of solutions in networks involving Hebbian learning, since the connectivity weights evolution depends on the firing correlations and the stability of the weights involves very similar equations as the ones we studied here.

The need for extensions of the present study to more realistic Markovian models involving more relevant biologically realistic transitions is a direct consequence of the present work. Indeed, we have seen that the transitions chosen in the Markovian model are only one-step jumps. In biological terms, this assumption means that when  $n_i(t)$  neurons are active in population at time  $i$ , at least  $n_i(t) - 1$  neurons are active at time  $t + dt$ , i.e. keep firing, which is not biologically realistic since after firing, a neuron immediately returns to quiescence. Therefore extending the framework to a more complex state space of the Markov chain would be of great interest for the development of these models towards more realistic biological grounds, and would probably allow a better assessment of the properties of cortical areas.

Finally, in order to go beyond the description of the moments of the Markov chain that are sometimes not sufficient to capture the behavior of the network we need to turn towards alternative ways to derive mean-field equations for such systems. A

particularly interesting way to study such systems we are currently exploring builds upon recent methods developed for the study of Markov chains, mainly in the field of queueing theory, such as fluid limits and large deviations approaches. The fluid limit technique is based on a space-time proper rescaling depending on the process under consideration, that yields deterministic or stochastic limits of the activity of the network when the number of neurons tends to infinity. Large deviation techniques allow one to derive the finite-size corrections (see e.g. [37] in a case of stochastic ion channels) and is a natural extension of our work.

**Acknowledgments:** This work was supported by NSF DMS 0817131.

**Appendix A. Markovian framework in details.** In the Markovian approach we consider in the paper, that each neuron can be either quiescent or active, active meaning in the process of firing an action potential. The ‘state’ of each neuron is equal to 0 if quiescent and 1 if active, and the state of the network is then described using the variable  $n \in \mathbb{N}^M$  where  $n_i(t)$  is defined by the total number of active neurons in population  $i$ . In the model considered, this variable constitutes a one-step discrete-time Markov process, i.e. the only possible transitions of this chain are assumed to be  $n_i \rightarrow n_i \pm 1$  for  $i \in \{1, \dots, M\}$ . This transition occurs by drawing from the transition probability of the chain, and this transition probability follows a differential equation called the *master equation*. This master equation can be written for complex models in a very general setting, as developed by El Boustani and Destexhe in [16], and one can extract from this differential equation the moments of the firing activity. However, the equations for the moments involve computing the expectation of a nonlinear function of the network state, which can itself be written as a sum over all the moments of the firing activity. At this point, one is led to truncate the expansion in the moments of the chain, in order to obtain closed equations only involving few moments.

In details, we denote by  $P(n, t)$  the probability that the network has configuration  $n$  at time  $t$ . The possible transitions  $n_i \rightarrow n_i + 1$  is governed by an activation function  $F_i$  depending on the population considered, on the synaptic weights  $W_{ij}$  and on the configuration of the network at time  $t$  (since it depends on the number of presynaptic spikes received by the neurons in the population). The transition  $n_i \rightarrow n_i - 1$  is related to the natural inactivation of neurons, and is governed by an inactivation function assumed to be proportional to the number of activated neurons in population  $i$  with a proportionality coefficient denoted  $\alpha_i$  independent of time and of the configuration of the network. In this framework, the master equation governing the transition probability of the network can be written as follows:

$$\frac{dP(n, t)}{dt} = \sum_{i=1}^M \left[ \alpha_i (n_i + 1) P(n_{i+}, t) - \alpha_i n_i P(n, t) \right. \\ \left. + F_i(n_{i-}) P(n_{i-}, t) - F_i(n) P(n, t) \right] \quad (\text{A.1})$$

where the configuration  $n_{i+}$  (resp.  $n_{i-}$ ) is the identical configuration as  $n$  except that  $n_i$  is incremented (resp. decremented) by one. This equation is complemented by the boundary conditions  $P(n, t) = 0$  if  $n_i = -1$  or  $n_i = N_i + 1$  for some  $i \in \{1, \dots, M\}$ .

This paper particularly focuses on two instances of this kind of models whose mean-firing rate is directly related to WC model: Buice, Cowan and Chow (BCC model, [12]) aimed at describing Poisson-like behaviors in neural populations, and Bressloff model ([7]) related to uncorrelated (asynchronous) activity.

Equation (A.1) is quite general and is globally the same for both BCC and

Bressloff models. However, these two models differ by the way they define the mean firing activity at the level of the populations, which depends on the phenomenon they want to study. Buice and collaborators specifically address the highly correlated modes of spiking in networks and where the statistics are Poisson-like. To this end, they define the firing activity of the population as the variable  $n$  directly, with no rescaling, which therefore allows the firing activity to be unbounded. In contrast, Paul Bressloff addresses the question of asynchronous states that are characterized by vanishing correlations of the firing activity in the limit  $N \rightarrow \infty$ . For this problem, it is particularly suitable to define the activity of the population through the variable  $\nu_i$  defined as the proportion of spiking neurons at time  $t$ :

$$\nu_i(t) = \frac{n_i(t)}{N_i}.$$

The activation function is not specified so far, and the choice of this function is driven by the constraint to recover WC equation for the mean firing activity in the limit where the number of neurons tends to infinity.

Let now derive the moment equations corresponding to a Markov chain with transition probability given by equation (A.1). From this equation, one can derive differential equations governing the moments of the activity variable  $n$ , which will be useful for both BCC and Bressloff models. We provide here closed-form expressions for the first three moments of such a Markov chain. For the sake of simplicity, we denote by  $\langle X \rangle$  the expectation of the variable  $X$  on all possible configurations of the network, and by  $a_i := \langle n_i \rangle$  the mean firing activity, by  $N_{ij} := \langle n_i(t) n_j(t) \rangle$  the correlations in the firing activity between different populations and by  $N_{ijk} := \langle n_i(t) n_j(t) n_k(t) \rangle$  the third moments. These moments will directly provide BCC's moments, and the expressions for Bressloff model involves a simple rescaling of these quantities since the firing activity is no more considered to be  $n_i$  but  $\nu_i = n_i/N_i$ .

LEMMA A.1. *The moments of the Markov process  $n$  governed by the master equation (A.1) satisfy the equations:*

$$\begin{cases} \frac{da_i}{dt} &= -\alpha_i a_i + \langle F_i \rangle \\ \frac{dN_{ij}}{dt} &= -(\alpha_i + \alpha_j) N_{ij} + \langle n_j F_i + n_i F_j \rangle + \langle F_i \rangle \delta_{ij} \\ \frac{dN_{ijk}}{dt} &= \begin{cases} -(\alpha_i + \alpha_j + \alpha_k) N_{ijk} + \langle n_i n_j F_k + n_i n_k F_j + F_i n_j n_k \rangle & \text{if } (i, j, k) \text{ pairwise distinct} \\ -(2\alpha_i + \alpha_k) N_{iik} + \alpha_i C_{ik} + \langle 2n_i n_k F_i + n_i^2 F_k \rangle + \langle n_k F_i \rangle & \text{if } i = j \neq k \\ -3\alpha_i N_{iii} + 3\alpha_i C_{ii} - \alpha_i a_i + 3\langle n_i^2 F_i \rangle + 3\langle n_i F_i \rangle + \langle F_i \rangle & \text{if } i = j = k \end{cases} \end{cases} \quad (\text{A.2})$$

*Proof.* The proof of this lemma consists in computing the expectations by summing over all possible configurations. For each moment computed, the proofs involve very similar arguments. We detail the derivation of the mean firing rate, and let the interested reader follow the paths of these calculations to derive the higher-order

moments given in the lemma. Since  $a_i(t) = \sum_n n_i P(n, t)$ , we have:

$$\begin{aligned} \frac{da_i}{dt} &= \sum_n n_i \frac{dP}{dt}(n, t) \\ &= \sum_{k=1}^N \sum_n n_i \left( \alpha_i ((n_k + 1)P(n_{k+}, t) - n_k P(n, t)) \right. \\ &\quad \left. + F_k(n_{k-})P(n_{k-}, t) - F_k(n)P(n, t) \right) \end{aligned}$$

For each  $k \neq i$  straightforward calculations show that the term in the sum vanishes by just reordering the terms and using the boundary conditions on  $P$ . Therefore, the only remaining term is the one corresponding to neuron  $i$ , and we get:

$$\begin{aligned} \frac{da_i}{dt} &= \sum_n n_i (\alpha_i ((n_i + 1)P(n_{i+}, t) - n_i P(n, t)) + F_i(n_{i-})P(n_{i-}, t) - F_i(n)P(n, t)) \\ &= \sum_n \alpha_i ((n_i - 1)n_i - n_i^2)P(n, t) + (n_i + 1 - n_i)F_i(n)P(n, t) \\ &= \sum_n -\alpha_i n_i P(n, t) + F_i(n)P(n, t) \\ &= -\alpha_i a_i + \langle F_i \rangle \end{aligned}$$

The correlation  $N_{ij} = \langle n_i(t) n_j(t) \rangle$  can be derived using the very same methods. We have for  $i \neq j$ :

$$\begin{aligned} \frac{dN_{ij}}{dt} &= \sum_n n_i n_j \frac{dP(n, t)}{dt} \\ &= \sum_n n_i n_j \left\{ \sum_{\beta=1}^M \sum_{k=1}^{N_\beta} \alpha_\beta (n_k + 1)P(n_{k+}, t) - \alpha_\beta n_k P(n, t) \right. \\ &\quad \left. + F_\beta(n_{k-})P(n_{k-}, t) - F_\beta(n_k)P(n, t) \right\} \end{aligned}$$

Developing this sum yields similar terms as in the computations done for the mean-firing rate. Most of these vanish, except for populations  $i$  and  $j$ , and direct computations yields the announced result.

□

REMARK Note that in this view, similarly to what was observed in [20], WC equations consist in commuting expectation and nonlinear sigmoidal transformation, i.e. identifying  $\langle F_i(n) \rangle$  and  $F_i(\langle n \rangle)$ , which is exact only if the state variable  $n$  is deterministic, or if  $F_i$  is affine (which is not the case). We also note that we only derived here the correlations of the firing activity at a given time  $t$ . The correlations at different times  $N_{ij}(t, s) = \langle n_i(t) n_j(s) \rangle$  are more difficult to derive, and though these can strongly impact solutions of the equations, they are neither used in BCC nor in Bressloff models. Rigorous derivation of the equation on the variable  $N_{ij}(s, t)$  would involve integral equations on the correlation that are way more complex to study than differential equations.

**A.1. BCC Model.** Buice, Cowan and Chow, interested in studying the Poisson-like firing modes of the network, transform the moment equations of lemma A.1 to provide equations on the *normal ordered cumulants* measuring the deviations of the moments of the variable  $n$  from pure Poisson statistics. From now on, we restrict our study to the two first moments of the firing activity. The first normal ordered cumulant is equal to  $a_i(t)$ , the second ordered cumulant to:

$$C_{ij} = N_{ij} - a_i a_j - a_i \delta_{ij}.$$

The transformed equations of (A.2) in terms of ordered cumulant read:

$$\begin{cases} \frac{da_i}{dt} &= -\alpha_i a_i + \langle F_i \rangle \\ \frac{dN_{ij}}{dt} &= -(\alpha_i + \alpha_j) N_{ij} + \langle (n_j - a_j) F_i + (n_i - a_i) F_j \rangle. \end{cases} \quad (\text{A.3})$$

At this point, they expand  $F_i$  in terms of their Taylor series and compute the expected values in terms of normal ordered cumulant. They make the assumption that  $\langle F_i \rangle = g_i(s_i) + \text{hot}$  where  $g$  is a sigmoidal function, similar to the one involved in Wilson and Cowan system, but that transforms activity into a total possibly unbounded firing rate as the population size increases, and with  $s_i = \sum_j W_{ij} a_j + I_i$ , and *hot* stands for higher order terms that depend on higher normal ordered cumulant. They end up with the following system of ordinary differential equations truncated to the second ordered cumulant:

$$\begin{cases} \frac{da_i}{dt} &= -\alpha_i a_i + g_i(s_i) + \frac{1}{2} g_i''(s_i) \sum_{j,k} W_{ij} W_{ik} C_{jk} \\ \frac{dC_{ij}}{dt} &= -(\alpha_i + \alpha_j) C_{ij} + g_i'(s_i) \sum_k W_{ik} C_{kj} \\ &\quad + g_j'(s_j) \sum_k W_{jk} C_{ki} + g_i'(s_i) W_{ij} a_j + g_j'(s_j) W_{ji} a_i \end{cases} \quad (\text{A.4})$$

The validity of this truncation is then proved when the system is far enough from bifurcations.

In order to implement our program of studying mean-field limit and finite-size effects in large networks, it is convenient to deal with quantities that remain bounded in the limit where the number of neurons tends to infinity. This is why we introduce a rescaling of the quantities involved, as we now describe in detail. First of all, in order for the global interaction statistics to be conserved, weights are to be normalized, and we define the interaction weight  $w_{ij}$  independent of the population size, such that  $W_{ij} = w_{ij}/N_j$  (this is similar to the rescaling done in a one-population case in [12]). In order define bounded mean-firing rates in the limit of large networks, we also rescale, similarly to Bressloff's approach, the activity  $a_i(t)$  by defining  $\nu_i(t) = a_i(t)/N_i$  and introducing rescaled correlation variables  $c_{ij} = C_{ij}/(N_i N_j)$ . With this rescaling, when a fraction of the neurons in a population fire, the total activity  $\nu_i$  will keep bounded, in contrast with the state variable  $n_i$  that produces an unbounded activity masking the effective activity of the population. In this same purpose, we eventually define the activity to rate transform  $f_i = g_i/N_i$  which is defined as the sigmoidal transform involved in WC system. Note that in this change of variable, we have the following identity:

$$s_i = \sum_{k=1}^M W_{ik} a_k = \sum_{k=1}^M \frac{w_{ik}}{N_k} a_k = \sum_{k=1}^M w_{ik} \nu_k$$

Using this change of variable, we obtain the following equations:

$$\begin{cases} \frac{d\nu_i}{dt} &= -\alpha_i \nu_i + f_i(s_i) + \frac{1}{2} g_i''(s_i) \sum_{j,k} w_{ij} w_{ik} c_{jk} \\ \frac{dc_{ij}}{dt} &= -(\alpha_i + \alpha_j) c_{ij} + f_i'(s_i) \sum_k w_{ik} c_{kj} + f_j'(s_j) \sum_k w_{jk} c_{ki} + \\ &\quad + \frac{1}{N_j} f_i'(s_i) w_{ij} \nu_j + \frac{1}{N_i} f_j'(s_j) w_{ji} \nu_i \end{cases}$$

We point out that these equations are particularly interesting for our study of mean-field limits and finite size effects, first of all because all quantities remain bounded in the mean-field limit and relate to the global mean activity of each population, and also because the size of the network appears in a very simple way as a parameter of the model. In particular, if considering  $n = 1/N$  as a continuous parameters, solutions will smoothly depend on  $n$ , and bifurcations can be studied as a function of this network size parameter. These equations are referred to as BCC equations in the main text.

**A.2. Bressloff Model.** We now turn to the Bressloff model. The basic framework is very similar to BCC's, and the methods to derive Bressloff's differential equations are closely related. The main distinction is that instead of considering the normal ordered cumulants, that are of particular interest when considering highly correlated (Poisson-like) activity, Bressloff only considers correlations of the firing activity, in order to specifically address asynchronous activity. In this model, Bressloff shows that the Taylor expansion of in the moment equations can be reduced using a moment hierarchy truncated with respect to power of the scaling parameter  $1/N$  (where  $N$  is the total number of neurons in each population, considered to be constant populationwise in Bressloff model). Considering the variables  $\nu_i = \langle n_i(t)/N \rangle$  and the correlation  $n_{ij}$  between  $n_i(t)/N$  and  $n_j(t)$ , Paul Bressloff derives the moment equations, and shows, using a sufficient condition to recover WC equations for the mean firing rate in the mean-field limit  $N \rightarrow \infty$ , that there is an indeterminacy in the activation function  $F_i$  which constitutes an infinite-dimensional degree of freedom for the choice of the nonlinear activity function  $F$ . This arbitrary choice can significantly affect the correlation equations while keeping the equation for the mean firing rates identical to WC equations in the limit where the number of neurons tends to infinity. Indeed, up to the second moment, the general Bressloff model equations read:

$$\begin{cases} \frac{d\nu_i}{dt} &= -\alpha_i \nu_i + f_i(s_i) + \frac{1}{2N_i} f_i''(s_i) \sum_{k,l} w_{ik} w_{il} n_{kl} \\ \frac{dn_{ij}}{dt} &= [a_i G_i(a) + H_i(a)] \delta_{i,j} - (\alpha_i + \alpha_j) n_{ij} \\ &\quad + \sum_k [f_i'(s_i) w_{ik} n_{kj} + f_j'(s_j) w_{jk} n_{ki}] \end{cases}$$

where

$$G_i(x) = 1 + \Gamma_i(x), \quad H_i(x) = f_i \left( \sum_{j=1}^M w_{ij} x_j \right) + x_i \Gamma_i(x)$$

and where  $\Gamma_i$  is an arbitrary positive function. Note that the rescaling of Bressloff equation related to the correlation is chosen to be  $1/N$ , where  $N$  in his case is the assumed constant number of neurons in each populations. When taking this function equal to zero following the choice of Bressloff, we obtain the following simple equations:

$$\begin{cases} \frac{d\nu_i}{dt} &= -\alpha_i \nu_i + f_i(s_i) + \frac{1}{2N} f_i''(s_i) \sum_{k,l} w_{ik} w_{il} n_{kl} \\ \frac{dn_{ij}}{dt} &= [\alpha_i \nu_i + f_i(s_i)] \delta_{i,j} - (\alpha_i + \alpha_j) n_{ij} \\ &\quad + \sum_k [f_i'(s_i) w_{ik} n_{kj} + f_j'(s_j) w_{jk} n_{ki}] \end{cases} \quad (\text{A.5})$$

where  $s_i = \sum_j w_{ij} \nu_j$ . Note that the rescaling choice in Bressloff's model (A.5) makes it difficult to study mean-field limits when the number of neurons tends to infinity and when the behavior is not an asynchronous state, because it is only rescaled by a factor  $1/N$ . Extending Bressloff's framework to populations having different number of neurons, we introduce the variable  $\nu_i = \langle n_i(t) \rangle / N_i$  and in order to get a proper rescaling on the correlations in the mean-field limit, we define  $C_{ij} = N_{ij} / (N_i N_j) - \nu_i \nu_j$ . These variables satisfy in Bressloff's framework the following equations:

$$\begin{cases} \frac{d\nu_i}{dt} &= -\alpha_i \nu_i + f_i(s_i) + \frac{1}{2} f_i''(s_i) \sum_{k,l} w_{ik} w_{il} C_{kl} \\ \frac{dC_{ij}}{dt} &= \frac{1}{N_i} [\alpha_i \nu_i + f_i(s_i)] \delta_{i,j} - (\alpha_i + \alpha_j) C_{ij} \\ &\quad + \sum_k [f_i'(s_i) w_{ik} C_{kj} + f_j'(s_j) w_{jk} C_{ki}] \end{cases}$$

**A.3. Equivalence of the two models.** We now show that up to the change of variable  $c_{ij} = C_{ij} - \nu_i / N_i \delta_{ij}$  in the Bressloff equations, the two models are equivalent up to a change of activation functions  $f_i$ . Starting from equations (A.5), we define  $h_{ij} = C_{ij} - \nu_i / N_i \delta_{ij}$ . We have:

$$\begin{aligned} \frac{d\nu_i}{dt} &= -\alpha_i \nu_i + f_i(s_i) + \frac{1}{2} f_i''(s_i) \sum_{k,l} w_{ik} w_{il} h_{kl} + \frac{1}{N_k} \nu_k \delta_{lk} \\ &= -\alpha_i \nu_i + \left( f_i(s_i) + \frac{\sum_l w_{il}}{2N} f_i''(s_i) (s_i - I_i) \right) + \frac{1}{2} f_i''(s_i) \sum_{k,l} w_{ik} w_{il} h_{kl} + \frac{1}{N_k} \nu_k \end{aligned}$$

which is equal to BCC equations up to the zeroth order in  $1/N$ . The equation on the correlations truncated to the first order in  $1/N$  reads:

$$\begin{aligned} \frac{dh_{ij}}{dt} &= -\frac{1}{N_i} \frac{d\nu_i}{dt} \delta_{ij} + \frac{1}{N_i} [\alpha_i \nu_i + f_i(s_i)] \delta_{i,j} - (\alpha_i + \alpha_j) C_{ij} + \sum_k [f_i'(s_i) w_{ik} C_{kj} + f_j'(s_j) w_{jk} C_{ki}] \\ &= \frac{1}{N_i} [\alpha_i \nu_i + f_i(s_i) + (\alpha_i \nu_i - f_i(s_i) - 2\alpha_i \nu_i) \delta_{i,j} - (\alpha_i + \alpha_j) h_{ij} \\ &\quad + \sum_k f_i'(s_i) w_{ik} (h_{kj} - \frac{1}{N_j} \nu_j \delta_{jk}) + \sum_k f_j'(s_j) w_{jk} (h_{ki} - \frac{1}{N_j} \nu_j \delta_{jk})] \\ &= -(\alpha_i + \alpha_j) h_{ij} + f_i'(s_i) \sum_k w_{ik} h_{kj} + f_j'(s_j) \sum_k w_{jk} h_{ki} + \\ &\quad + \frac{1}{N_j} f_i'(s_i) w_{ij} \nu_j + \frac{1}{N_i} f_j'(s_j) w_{ji} \nu_i \end{aligned}$$

Therefore, the two models can be seen as a transformation of the one to the other through a change of variables and truncation of the equations at different orders in  $1/N$ . The change of variables tends to identity as the network size increases, yielding for both models the infinite-size system described in the main text.

**Appendix B. Kronecker Algebra: Some useful properties.** In this appendix, we review and prove some useful properties of Kronecker products of matrixes. We recall the definition of the the function *Vect* transforming a  $M \times N$  matrix into a  $MN$ -dimensional column vector, as defined in [29]:

$$\text{Vect} : \begin{cases} \mathbb{R}^{M \times N} & \mapsto \mathbb{R}^{MN} \\ X & \mapsto [X_{11}, \dots, X_{M1}, X_{12}(t), \dots, X_{M2}(t), \dots, X_{1N}(t), \dots, X_{MN}(t)]^T \end{cases}$$

Let us now denote by  $\otimes$  the Kronecker product defined for  $A \in \mathbb{R}^{m \times n}$  and  $B \in \mathbb{R}^{r \times s}$  as the  $(mr) \times (ns)$  matrix:

$$A \otimes B := \begin{pmatrix} a_{11}B & a_{12}B & \cdots & a_{1n}B \\ a_{21}B & a_{22}B & \cdots & a_{2n}B \\ \vdots & \vdots & \ddots & \vdots \\ a_{m1}B & a_{m2}B & \cdots & a_{mn}B \end{pmatrix}$$

For standard definitions and identities in the field of Kronecker products, the reader is referred to [8]. We recalled in the main text the following identities for  $A, B, D, G, X \in \mathbb{R}^{M \times M}$ ,  $I_M$  be the  $M \times M$  identity matrix and  $A \cdot B$  or  $AB$  denote the standard matrix product:

$$\begin{cases} Vect(AXB) = (B^T \otimes A)Vect(X) \\ A \oplus A = A \otimes I_M + I_M \otimes A \\ (A \otimes B) \cdot (D \otimes G) = (A \cdot D) \times (B \cdot G) \end{cases} \quad (\text{B.1})$$

The relationship  $\oplus$  is called Kronecker sum.

PROPOSITION B.1. *Let  $A$  and  $B$  in  $\mathbb{R}^{M \times M}$ , and assume that  $A$  has the eigenvalues  $\{\lambda_i; i = 1, \dots, M\}$  and  $B$  the eigenvalues  $\{\mu_i; i = 1, \dots, M\}$ . Then we have:*

- $A \otimes B$  has the eigenvalues  $\{\lambda_i \mu_j; (i, j) \in \{1, \dots, M\}^2\}$ .
- $A \oplus B$  has the eigenvalues  $\{\lambda_i + \mu_j; (i, j) \in \{1, \dots, M\}^2\}$ .

*Proof.* Let  $\lambda_i$  (resp.  $\mu_j$ ) be an eigenvalue of  $A$  (resp.  $B$ ) with eigenvector  $u$  (resp.  $v$ ), and define the matrix  $z = u \cdot v^T$  (i.e.  $z_{ij} = u_i v_j$ ). We have:

$$\begin{aligned} (A \oplus B) Vect(z) &= Vect(A \cdot u \cdot v^T + u \cdot v^T \cdot B^T) \\ &= Vect(\lambda_i u \cdot v^T + u \cdot (B \cdot v)^T) \\ &= \lambda_i Vect(z) + Vect(u(\mu_j v^T)) \\ &= (\lambda_i + \mu_j) Vect(z). \end{aligned}$$

which entails that  $Vect(z)$  is an eigenvector of  $A(\nu) \oplus A(\nu)$  associated with the eigenvalue  $\lambda_i + \lambda_j$ . Similarly, we have for  $z = v \cdot u^T$ :

$$\begin{aligned} (A \otimes B) Vect(z) &= Vect(B \cdot v \cdot u^T A^T) \\ &= Vect((\mu_j v) \cdot (\lambda_i u^T)) \\ &= \lambda_i \mu_j Vect(z) \end{aligned}$$

The dimension of  $A \oplus B$  and  $A \otimes B$  is  $M^2$  and there are exactly  $M^2$  linearly independent matrices  $z$  possible built in the proposed fashion, therefore we identified all possible eigenvalues.  $\square$

THEOREM B.2. *Let  $\Phi(t)$  be the solution of the matrix differential equation:*

$$\begin{cases} \frac{d\Phi(t)}{dt} = A(t)\Phi(t) \\ \Phi(0) = I_M \end{cases}$$

and  $\Psi(t)$  the solution of:

$$\begin{cases} \frac{d\Psi(t)}{dt} = (A(t) \oplus A(t))\Psi(t) \\ \Psi(0) = I_{M^2} \end{cases}$$

We have  $\Psi(t) = \Phi(t) \otimes \Phi(t)$ .

*Proof.* Indeed, we have, using the basic properties of the Kronecker product recalled in equation (2.1)

$$\begin{aligned}
\frac{d\Phi(t) \otimes \Phi(t)}{dt} &= \frac{d\Phi(t)}{dt} \otimes \Phi(t) + \Phi(t) \otimes \frac{d\Phi(t)}{dt} \\
&= (A(\nu(t)) \cdot \Phi(t)) \otimes \Phi(t) + \Phi(t) \otimes (A(\nu(t)) \cdot \Phi(t)) \\
&= (A(\nu(t)) \cdot \Phi(t)) \otimes (I_M \cdot \Phi(t)) + (I_M \cdot \Phi(t)) \otimes (A(\nu(t)) \cdot \Phi(t)) \\
&= (A(\nu(t)) \otimes I_M) \cdot (\Phi(t) \otimes \Phi(t)) + (I_M \otimes A(\nu(t))) \cdot (\Phi(t) \otimes \Phi(t)) \\
&= (A(\nu(t)) \otimes I_M + I_M \otimes A(\nu(t))) \cdot (\Phi(t) \otimes \Phi(t)) \\
&= (A(\nu(t)) \oplus A(\nu(t))) \cdot (\Phi(t) \otimes \Phi(t))
\end{aligned}$$

Therefore  $\Phi(t) \otimes \Phi(t)$  satisfies the same differential equation as  $\Psi(t)$  and moreover,  $\Phi(0) \otimes \Phi(0) = I_M \otimes I_M = I_{M^2}$ , and therefore by existence and uniqueness of the resolvent,  $\Psi(t) = \Phi(t) \otimes \Phi(t)$ .  $\square$

**Appendix C. Genericity of the Hopf bifurcation found.** In this appendix we derive the expression of the first Lyapunov exponent of the bifurcation, which proves that the existence of the Hopf bifurcation exhibited in section 3.1.2. In that section, we derived the expression of the Jacobian matrix at the considered fixed point:

$$J = \begin{pmatrix} -\alpha + w f'(s) & \frac{1}{2} f''(s) w^2 \\ 2f'(s) \frac{w}{N} & 2(-\alpha + w f'(s)) \end{pmatrix}$$

At the bifurcation point, we have  $-\alpha^* + w f'(s) = 0$ , and therefore at this point the Jacobian matrix reads:

$$J_0 = \begin{pmatrix} 0 & \frac{1}{2} f''(I) w^2 \\ 2f'(I) \frac{w}{N} & 0 \end{pmatrix}$$

The eigenvalues of this matrix under the assumptions of section 3.1.2 are  $\pm i\omega_0$  where  $\omega_0 = \sqrt{-f'(I)f''(I)w^3/N}$ . We define  $q$  the right eigenvector of  $J_0$  associated with  $i\omega_0$ :

$$q = \left( -\frac{i}{\sqrt{2 f'(I) w/N}} \quad 1 \right)^T$$

and  $p$  the right eigenvector of  $J_0^T$  associated with the eigenvalue  $i\omega_0$ :

$$p = \left( \frac{i}{\sqrt{-\frac{1}{2} f''(I) w^2}} \quad 1 \right)^T$$

For the sake of simplicity, we also name the components of the vector field of the system:

$$\begin{cases} f_1\left(\begin{pmatrix} \nu \\ C \end{pmatrix}, \alpha^*\right) &= w f'(I) n u + f(w\nu + I) + \frac{1}{2} f''(w\nu + I) w^2 C \\ f_2\left(\begin{pmatrix} \nu \\ C \end{pmatrix}, \alpha^*\right) &= -2 w f'(I) C + 2 f'(w\nu + I) w \left( C + \frac{\nu}{N} \right) \end{cases}$$

Following [24], we define  $B\left(\begin{pmatrix} x_1 \\ y_1 \end{pmatrix}, \begin{pmatrix} x_2 \\ y_2 \end{pmatrix}\right)$  and  $C\left(\begin{pmatrix} x_1 \\ y_1 \end{pmatrix}, \begin{pmatrix} x_2 \\ y_2 \end{pmatrix}, \begin{pmatrix} x_3 \\ y_3 \end{pmatrix}\right)$  the second and third derivatives of the vector field, which are bi- and tri-linear forms. We have the following expressions for these multilinear functions:

$$\begin{cases} B_1\left(\begin{pmatrix} x_1 \\ y_1 \end{pmatrix}, \begin{pmatrix} x_2 \\ y_2 \end{pmatrix}\right) &= w^2 f''(I) x_1 x_2 + \frac{1}{2} f''(I) w^2 (x_1 y_2 + y_1 x_2) \\ B_2\left(\begin{pmatrix} x_1 \\ y_1 \end{pmatrix}, \begin{pmatrix} x_2 \\ y_2 \end{pmatrix}\right) &= 2 f''(I) w^2 (x_1 y_2 + y_1 x_2) + \frac{4}{N} f''(I) w^2 x_1 x_2 \\ C_1\left(\begin{pmatrix} x_1 \\ y_1 \end{pmatrix}, \begin{pmatrix} x_2 \\ y_2 \end{pmatrix}, \begin{pmatrix} x_3 \\ y_3 \end{pmatrix}\right) &= f^{(3)}(I) w^3 x_1 x_2 x_3 + \frac{1}{2} f^{(4)}(I) w^4 (x_1 x_2 y_3 + x_1 y_2 x_3 + y_1 x_2 x_3) \\ C_2\left(\begin{pmatrix} x_1 \\ y_1 \end{pmatrix}, \begin{pmatrix} x_2 \\ y_2 \end{pmatrix}, \begin{pmatrix} x_3 \\ y_3 \end{pmatrix}\right) &= \frac{6}{N} f^{(3)}(I) w^3 x_1 x_2 x_3 + 2 f^{(3)}(I) w^3 (x_1 x_2 y_3 + x_1 y_2 x_3 + y_1 x_2 x_3) \end{cases}$$

We are now in position to compute the first Lyapunov exponent  $l_1(0)$  using the formula:

$$\begin{aligned} l_1(0) &= \frac{1}{2\omega_0} \operatorname{Re} \left( \langle p, C(q, q, \bar{q}) \rangle - 2 \langle p, B(q, J_0^{-1} B(q, \bar{q})) \rangle + \langle p, B(\bar{q}, (2i\omega_0 Id - J_0)^{-1} B(q, q)) \rangle \right) \\ &= \frac{1}{2\omega_0} (\mathcal{A} - 2\mathcal{B} + \mathcal{C}) \end{aligned}$$

where  $\langle x, y \rangle$  denotes the complex inner product  $\bar{x}^T \cdot y$  and the sum of three terms denoted  $\mathcal{A}$ ,  $\mathcal{B}$  and  $\mathcal{C}$  are the real parts of the terms involved in the expression of the Lyapunov exponent. After straightforward but tedious calculations (that can be conveniently performed using a formal calculation tool such as Maple), we obtain:

$$\begin{cases} \mathcal{A} &= \frac{w^2 N}{f'(I)^2} f^{(3)}(I) f'(I) \\ \mathcal{B} &= \frac{w^2 N}{f'(I)^2} \left( -\frac{f''(I)^2}{\omega_0} - \frac{1}{2} \frac{f^{(3)}(I) f'(I)}{\omega_0} + 2f''(I)^2 \right) \\ \mathcal{C} &= -\frac{w^2 N}{f'(I)^2} \frac{2f''(I)^2}{3} \end{cases}$$

which yields the expression for the Lyapunov exponent:

$$\begin{aligned} l_1(0) &= \frac{1}{2\omega_0} [\mathcal{A} - 2\mathcal{B} + \mathcal{C}] \\ &= \frac{w^2 N}{2\omega_0 f'(I)^2} \left[ f^{(3)}(I) f'(I) \left( 1 + \frac{1}{\omega_0} \right) + f''(I)^2 \left( \frac{2}{\omega_0} - \frac{14}{3} \right) \right] \end{aligned}$$

#### Appendix D. Finite-size effects in Buice and Cowan two-populations

**Model I.** In this appendix, we study the two-populations Buice and Cowan system corresponding to Model I and show that the finite-size effects are closely related to what is observed in Bressloff model as studied in section 3.2. BCC finite-size equations read:

$$\begin{cases} a'_1 &= -\alpha a_1 + f(s_1) + \frac{1}{2} f''(s_1) (w_{11}^2 c_{11} + w_{12}^2 c_{22} + 2 w_{12} w_{11} c_{12}) \\ a'_2 &= -\alpha a_2 + f(s_2) + \frac{1}{2} f''(s_2) (w_{22}^2 c_{22} + w_{21}^2 c_{11} + 2 w_{22} w_{21} c_{12}) \\ c'_{11} &= -2\alpha c_{11} + 2 f'(s_1) (w_{11} c_{11} + w_{12} c_{12}) + 2 f'(s_1) a_1 w_{11} n_e \\ c'_{22} &= -2\alpha c_{22} + 2 f'(s_2) (w_{21} c_{12} + w_{22} c_{22}) + 2 n_i f'(s_2) w_{22} a_2 \\ c'_{12} &= -2\alpha c_{12} + f'(s_1) (w_{11} c_{12} + w_{12} c_{22} + a_2 w_{12} n_i) \dots \\ &\quad + f'(s_2) (w_{21} c_{11} + w_{22} c_{12} + w_{21} a_1 n_e) \end{cases} \quad (\text{D.1})$$

where we denoted:

$$\begin{cases} s_1 &= w_{11} a_1 + w_{12} a_2 + i_1 \\ s_2 &= w_{21} a_2 + w_{22} a_2 + i_2 \end{cases}$$

Similarly to Bressloff case, BCC model features two families of limit cycles. One of these branches corresponds exactly to the branch of limit cycles of WC system starting from a Hopf bifurcation and disappearing through a saddle-node homoclinic bifurcations. Two additional Hopf bifurcations appear related to the family of periodic orbit corresponding to the correlation-induced cycle evidence in the analysis of the infinite-size system. This branch of limit cycles exist whatever  $n$ , and loses stability through a Neimark-Sacker bifurcation as the number of neurons increases. This bifurcation generates chaos for large enough networks, which clearly does not exists in WC system.

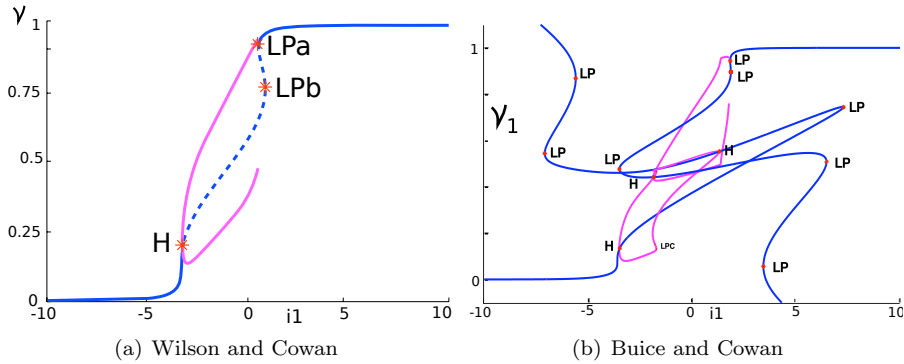
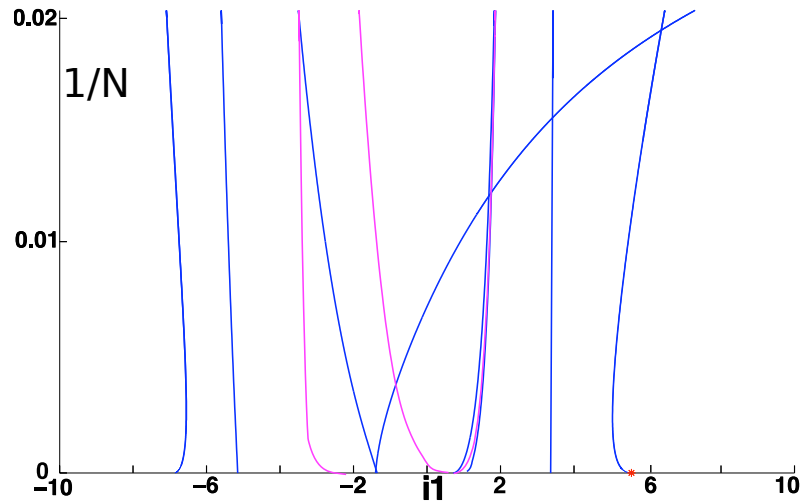


FIG. D.1. Bifurcation diagram for the Buice and Cowan system. Blue lines represent the equilibria, pink lines the extremal values of the cycles in the system. Bifurcations of equilibria are denoted with a red star, LP represents a saddle-node bifurcation (Limit Point), H a Hopf bifurcation. The four Hopf bifurcations share two families of limit cycles. The branch corresponding to the smaller values of  $i_1$  undergoes two fold of limit cycles, and the other branch of limit cycle a Neimark Sacker (Torus) bifurcation.

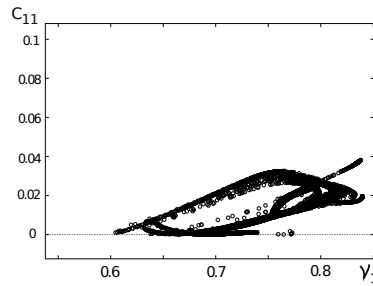
This family of limit cycles presents stability for networks containing between 100 and 17.000 neurons, corresponding to a finite size effect that appears only in the region of interest of the cortical columns. As the number of neurons increase, the system keep the same number and type of bifurcations, and the infinite model appears to be a singular case where different bifurcations meet (see Fig. D.2), and very large networks lose the property of presenting a stable cycle, and present a chaotic behavior.

#### REFERENCES

- [1] L.F. ABBOTT AND C.A. VAN VREESWIJK, *Asynchronous states in networks of pulse-coupled neuron*, Phys. Rev, 48 (1993), pp. 1483–1490.
- [2] S. AMARI, *Characteristics of random nets of analog neuron-like elements*, Syst. Man Cybernet. SMC-2, (1972).
- [3] S.-I. AMARI, *Dynamics of pattern formation in lateral-inhibition type neural fields*, Biological Cybernetics, 27 (1977), pp. 77–87.
- [4] D.J. AMIT AND N. BRUNEL, *Model of global spontaneous activity and local structured delay activity during delay periods in the cerebral cortex*, Cerebral Cortex, 7 (1997), pp. 237–252.
- [5] JOHN M BEGGS AND DIETMAR PLENZ, *Neuronal avalanches are diverse and precise activity patterns that are stable for many hours in cortical slice cultures.*, J Neurosci, 24 (2004), pp. 5216–5229.
- [6] MARC BENAYOUN, JACK D. COWAN, WIM VAN DRONGELEN, AND EDWARD WALLACE, *Avalanches in a stochastic model of spiking neurons*, PLoS Comput Biol, 6 (2010/07/08), pp. e1000846–



(a) Codimension 2 bifurcations



(b) The stable cycle yielding chaos

FIG. D.2. Codimension two bifurcations and chaotic behavior as the number of neuron increases.

- [7] PAUL BRESSFLOFF, *Stochastic neural field theory and the system-size expansion*. Submitted, 2009.
- [8] JOHN BREWER, *Kronecker Products and Matrix Calculus in System Theory*, IEEE Trans. Circuits Syst., CAS-25 (1978).
- [9] N. BRUNEL, *Dynamics of sparsely connected networks of excitatory and inhibitory spiking neurons*, Journal of Computational Neuroscience, 8 (2000), pp. 183–208.
- [10] N. BRUNEL AND V. HAKIM, *Fast global oscillations in networks of integrate-and-fire neurons with low firing rates*, Neural Computation, 11 (1999), pp. 1621–1671.
- [11] N BRUNEL AND P LATHAM, *Firing rate of noisy quadratic integrate-and-fire neurons*, Neural Computation, 15 (2003), pp. 2281–2306.
- [12] M.A. BUICE, J.D. COWAN, AND C.C. CHOW, *Systematic fluctuation expansion for neural network activity equations*, Arxiv preprint arXiv:0902.3925, (2009).
- [13] D CAI, L TAO, M SHELLEY, AND DW MCLAUGHLIN, *An effective kinetic representation of fluctuation-driven neuronal networks with application to simple and complex cells in visual cortex*, Proceedings of the National Academy of Sciences, 101 (2004), pp. 7757–7762.
- [14] S. COOMBES AND M. R. OWEN, *Bumps, breathers, and waves in a neural network with spike frequency adaptation*, Phys. Rev. Lett., 94 (2005).
- [15] JL DOOB, *Markoff chains—denumerable case*, Transactions of the American Mathematical Society, 58 (1945), pp. 455–473.
- [16] S EL BOUSTANI AND A DESTEXHE, *A master equation formalism for macroscopic modeling of*

- asynchronous irregular activity states*, *Neural computation*, 21 (2009), pp. 46–100.
- [17] BARD ERMENTROUT, *Neural networks as spatio-temporal pattern-forming systems*, *Reports on Progress in Physics*, 61 (1998), pp. 353–430.
- [18] B. ERMENTROUT, *Simulating, Analyzing, and Animating Dynamical Systems: A Guide to XPPAUT for Researchers and Students*, Society for Industrial Mathematics, 2002.
- [19] G B ERMENTROUT AND J D COWAN, *A mathematical theory of visual hallucination patterns.*, *Biol Cybern*, 34 (1979), pp. 137–150.
- [20] O. FAUGERAS, J. TOUBOUL, AND B. CESSAC, *A constructive mean field analysis of multi population neural networks with random synaptic weights and stochastic inputs*, *Frontiers in Neuroscience*, 3 (2009).
- [21] DT GILLESPIE, *A general method for numerically simulating the stochastic time evolution of coupled chemical reactions*, *Journal of computational physics*, 22 (1976), pp. 403–434.
- [22] ———, *Exact stochastic simulation of coupled chemical reactions*, *The journal of physical chemistry*, 81 (1977), pp. 2340–2361.
- [23] J. GUCKENHEIMER AND P. J. HOLMES, *Nonlinear Oscillations, Dynamical Systems and Bifurcations of Vector Fields*, vol. 42 of Applied mathematical sciences, Springer, 1983.
- [24] YURI A. KUZNETSOV, *Elements of Applied Bifurcation Theory*, Applied Mathematical Sciences, Springer, 2nd ed., 1998.
- [25] C.L. LAING, W.C. TROY, B. GUTKIN, AND G.B. ERMENTROUT, *Multiple bumps in a neuronal model of working memory*, *SIAM J. Appl. Math.*, 63 (2002), pp. 62–97.
- [26] ANNA LEVINA, J. MICHAEL HERRMANN, AND THEO GEISEL, *Phase transitions towards criticality in a neural system with adaptive interactions*, *Phys. Rev. Lett.*, 102 (2009).
- [27] CHENG LY AND DANIEL TRANCHINA, *Critical analysis of dimension reduction by a moment closure method in a population density approach to neural network modeling.*, *Neural Computation*, 19 (2007), pp. 2032–2092.
- [28] M. MATTIA AND P. DEL GIUDICE, *Population dynamics of interacting spiking neurons*, *Physical Review E*, 66 (2002), p. 51917.
- [29] H NEUDECKER, *Some theorems on matrix differentiation with special reference to kronecker matrix products*, *Journal of the American Statistical Association*, 64 (1969), pp. 953–963.
- [30] H. E. PLESSER, *Aspects of signal processing in noisy neurons*, PhD thesis, Georg-August-Universität, 1999.
- [31] R RODRIGUEZ AND H C TUCKWELL, *Noisy spiking neurons and networks: useful approximations for firing probabilities and global behavior.*, *Biosystems*, 48 (1998), pp. 187–194.
- [32] ET ROLLS AND G DECO, *The noisy brain: stochastic dynamics as a principle of brain function*, Oxford university press, 2010.
- [33] WILLIAM R. SOFTKY AND CHRISTOF KOCH, *The highly irregular firing of cortical cells is inconsistent with temporal integration of random epsps*, *Journal of Neuroscience*, 13 (1993), pp. 334–350.
- [34] J. TOUBOUL AND A. DESTEXHE, *Can power-law scaling and neuronal avalanches arise from stochastic dynamics?*, *PLoS ONE*, 5 (2010), p. e8982.
- [35] JONATHAN TOUBOUL AND OLIVIER FAUGERAS, *The spikes trains probability distributions: a stochastic calculus approach*, *Journal of Physiology, Paris*, 101/1-3 (2007), pp. 78–98.
- [36] ———, *First hitting time of double integral processes to curved boundaries*, *Advances in Applied Probability*, 40 (2008), pp. 501–528.
- [37] GILLES WAINRIB, *Randomness in Neurons: a multiscale probabilistic analysis*, PhD thesis, Ecole Polytechnique, 2010.
- [38] H.R. WILSON AND J.D. COWAN, *Excitatory and inhibitory interactions in localized populations of model neurons*, *Biophys. J.*, 12 (1972), pp. 1–24.
- [39] H.R. WILSON AND J.D. COWAN, *A mathematical theory of the functional dynamics of cortical and thalamic nervous tissue*, *Biological Cybernetics*, 13 (1973), pp. 55–80.